March 2019

Determination of Conversion Factors for Various Calibration Geometries using Barium-133 in a Silver Zeolite Cartridge

Amin Hamideh
ahamid1@lsu.edu

DETERMINATION OF CONVERSION FACTORS FOR VARIOUS CALIBRATION GEOMETRIES USING BARIUM-133 AS A SURROGATE FOR GASEOUS IODINE-131 IN A SILVER ZEOLITE CARTRIDGE.

A Thesis

Submitted to the Graduate faculty of the
Louisiana State University and
Agricultural and Mechanical College
in partial fulfillment of the
requirements for the degree of
Master of Science

in

The Department of Physics and Astronomy

by
Amin Munther Hamideh
B.S., B.S., Louisiana State University, 2007 and 2012
May 2019

ACKNOWLEDGEMENTS

First, I thank my master's thesis committee for their help and guidance during this process. Dr. Wei-Hsung Wang was with me all the way as my mentor, thesis advisor and boss at the Radiation Safety Office. He knew that one of my main research interests is in air sampling and provided me with the principal idea and direction for this project. I am also grateful to all my committee members: Dr. Kenneth Matthews, Dr. Scott Marley, and Dr. Slawomir Lomniki for vital technical advice, especially with the analysis of data.

I also thank Michael McMahon at the Louisiana Department of Environmental Quality for providing me technical guidance on the calibration of sodium iodide detectors using charcoal and silver zeolite cartridges, and emergency response protocols during a potential nuclear incident in the State of Louisiana. Also, I would like to thank my coworkers at the Radiation Safety Office, Jabari Robinson and Charles Wilson, for helping me with regulatory, experimental design and statistical questions. And also, Melissa Esnault for providing editorial comments and feedback on this paper.

In addition, I thank the Louisiana Sea Grant office at Louisiana State University for funding this research. This project could not have been started without their help. I hope to continue working closely with them on future projects related to this research.

Also, and most importantly, I thank my family. Especially my wife, Sharifeh, for being patient with me during these last couple of years. She has supported me through this whole process and stuck close to me. I also thank my children, Karam and Ayat. After a long day of hard work, it's nice to come home and play with them. This was a great stress reliever. Also, my parents Munther and Nadua for supporting me throughout my academic career. They have always shown an interest in my school work and research and I could not have made it without

them. Finally, my grandparents Abdel-Karim and Eli Hamideh, who have also supported me and took great interest in my school work as well. Their loving care will never be forgotten.

TABLE OF CONTENTS

ABSTRACT

Iodine-131 (I-131) is a major fission product among other radionuclides released during a nuclear incident. This radioiodine has a half-life of 8.02 days and the primary organ of uptake through ingestion or inhalation is the thyroid gland. For these reasons, nuclear power plants must routinely monitor I-131 through air sampling. Currently, there are two adsorbing media to collect I-131: activated charcoal and silver zeolite cartridges. Silver zeolite cartridges are generally used during a post nuclear incident due to its affinity for iodine while not adsorbing noble gases such as krypton-85 and xenon-135. After an air sample is taken from a plume, the cartridge is taken to a low radiation background area for measuring the radioactivity of I-131. This is usually done by using a γ-spectroscopy detection system. To use these detectors, the system must be calibrated using the same source geometry as in the field. Source geometry refers to source to detector orientation when counting. Because of licensing issues, radiation protection problems, and financial concerns, many agencies or institutions use a single barium-133 (Ba-133) sealed point source on top of a silver zeolite cartridge as their calibration standard for air sampling purposes. This method does not reflect the actual gaseous I-131 distribution in the silver zeolite cartridge. Consequently, the ambient gaseous I-131 activity would be underestimated due to different source geometries/counting efficiencies. This study compares various geometrical arrangements of both Ba-133 and I-131 spiked filter media in a silver zeolite cartridge to mimic the gaseous I-131 distribution found in the field in order to establish conversion factors back to a Ba-133 sealed point source geometry for proper calibration of a sodium iodide detection system based on their counting efficiencies. The results of this study demonstrate that nine is the best correction factor for estimating I-131 activity measured in the field using a Ba-133 sealed point source for calibration.

CHAPTER 1. DETERMINING IODINE-131 CONCENTRATIONS AFTER A NUCLEAR INCIDENT

1.1. Iodine-131 and Barium-133

Iodine-131 (I-131), as well as other radioisotopes of iodine, is a major fission product released from nuclear power plant during a nuclear incident. This radionuclide has a physical half-life of 8.02 days and its primary decay emissions are both a beta particle (606 keV β, 89%) and a gamma ray (364 keV γ, 81.5%) to stable xenon-131 (Radionuclide Safety Data Sheet, 2019). The primary concern with this radionuclide when released into the environment is the internal effects if ingested or inhaled. Once I-131 enters the body, the radionuclide can be absorbed into the thyroid gland of humans, which is the primary organ of iodine uptake in mammals (Jiemwutthisak *et al*., 2012). Although the physical half-life is only 8.02 days, I-131 has a biological half-life of approximately 130 days. The thyroid gland uses iodine as an important cofactor in the development of several hormones, primarily thyroxine (T4) and triiodothyronine (T3) in the body that control various metabolic processes (Jiemwutthisak *et al*., 2012). Therefore, due to the sensitivity of the thyroid in the normal functioning of the human body, minimizing any chances of radioiodine to be incorporated within the organ is essential for human metabolism and development. In addition, I-131 can affect the soil, vegetation, wildlife and fisheries. Internal contamination results from ingestion of food, drinking water, and dust and/or soil inhalation. During a nuclear incident, I-131 is released into the atmosphere by a plume cloud which is known as fallout. The fallout drops from the atmosphere and is then settled on top of the soil where it is taken up. Plants then absorb this fallout from the soil. Iodine-131 is then distributed throughout the plant to its vegetation. Grazing animals then feed on these plants where I-131 is ingested. The I-131 is then incorporated into the milk and meat of grazing animals. Also, fish ingest the water and soil resulting in incorporation of I-131. The importance

of determining the activity of I-131 is equally important in Louisiana due to the state having three nuclear power plants located in close approximation to the Gulf of Mexico: Riverbend Nuclear Power Plant in St. Francisville, LA, Waterford 3 Nuclear Generating Station in Killona, LA, and Grand Gulf Nuclear Station in Port Gibson, MS. The U.S. Nuclear Regulatory Agency (U.S. NRC) and U.S. Environmental Protection Agency (EPA) have established many regulations and guidelines to decrease the chances of ingestion or inhalation of radioiodine (EPA-PAG, 2017 and NUREG-0654, 1980). To comply with these regulations and/or guidelines, nuclear power plants are required to routinely monitor the emission of several fission products from its stacks, especially I-131 (NUREG-0654, 1980). During a post-nuclear incident, an emergency response team is called out (typically the state's regulatory agency) and takes air samples using calibrated air samplers usually at a location inward of the plume (FEMA-RAAC, 2019). Once the air sample is taken for a pre-established time, the cartridge is taken to a low radiation background area and counted using a variety of radioanalytical equipment (Maiello and Hoover, 2011). The calculated activity is then divided by the volume of air taken within the pre-established time of the air sample to get a radioisotope concentration, typically $\mu Ci/cm^3$. This concentration is then converted to a dose equivalent using specialized software and algorithms such as RASCAL®. These dose equivalents determine the actions needed to be taken by the State for evacuation, distribution of potassium iodide (KI), and shelter in place according to the EPA-Protective Action Guides (EPA-PAG's, 2017). Currently, there are two popular absorbing media for monitoring radioiodines in a plume using air samplers; activated charcoal and silver zeolite (AgZ) cartridges (Wang and Matthews, 2006). In 2006, Wang and Matthews published a paper in Operational Radiation Safety of the Health Physics Journal, "Developing a methodology to simulate gaseous ^{131}I distribution in a silver zeolite cartridge using liquid ^{131}I". This approach

was desirable because of the simplicity and accuracy in preparing a calibration standard for I-131. Though, because of licensing issues, radiation protection problems, and financial concerns, most agencies or institutions still use a barium-133 (Ba-133) sealed point or planar source on top of a silver zeolite cartridge as their calibration standard to determine I-131 activity. Iodine-131 is exempt from the U.S. NRC up to 37 kBq (1 μCi) and many radioisotope distributers do not make this low quantity of material (most start producing I-131 at 37 MBq (1 mCi)). This also includes total quantity in possession. A larger activity of I-131 would warrant the application of a radioactive materials license from either the U.S. NRC or state regulatory agency. Iodine-131 has many radiation protection concerns. For instance, does the institution have an appropriate laboratory for the use of radioactive materials? Using I-131 requires a properly calibrated hood in terms of face velocity, shielding, radioactive waste disposal, and radiation monitoring equipment. Financial concerns come from the short half-life of I-131 (8.02 days). The institution may find themselves having to frequently order I-131 for calibration purposes and can cost up to $200 per 37 MBq (1 mCi). Barium-133 has a half-life of 10.5 years and its primary decay emissions are both a beta particle (80.4 keV β, 86%) and a gamma ray (356 keV γ, 62%) to stable cesium-133 (Radionuclide Data Sheet, 2019). Due to its long half-life, primary gamma emission energy close to that of I-131 and exempted up to 370 MBq (10 uCi) by the U.S. NRC, makes it an attractive alternative as a calibration standard.

Table 1.1. Protective Action Guides showing dose equivalents for the Early Phase of a nuclear incident. Taken from EPA-PAG's, 2017

Phase	Protective Action Recommendation	Planning Guidance
Early Phase	Sheltering-in-place or evacuation of the public	PAG: 10 to 50 mSv
	Administration of potassium iodide (KI)	PAG: 50 mSv for children thyroid dose
	Limit emergency worker exposure	PAG: 50 mSv/year

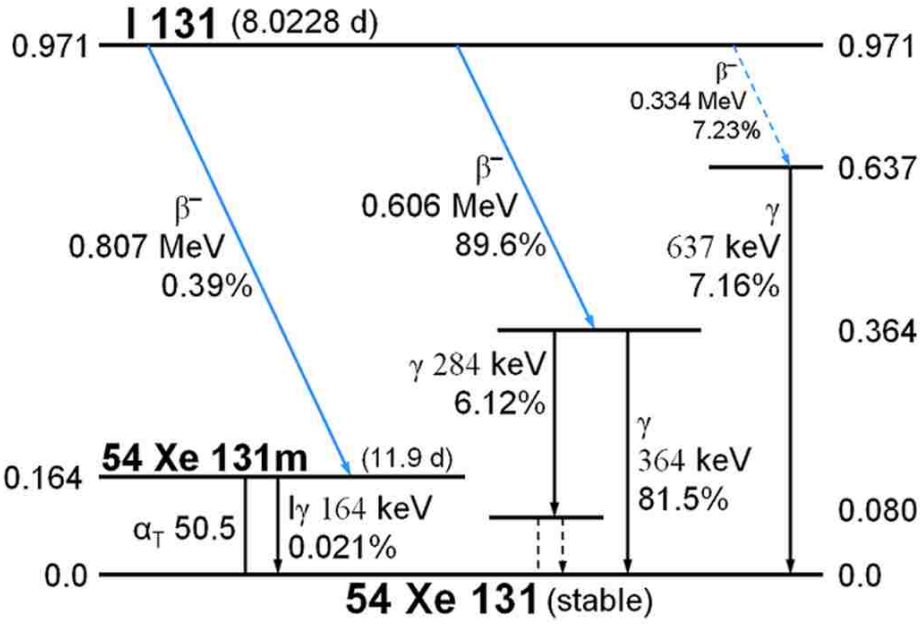

Figure 1.1. Figure of I-131 decay scheme. Taken from Nucleonica.com.

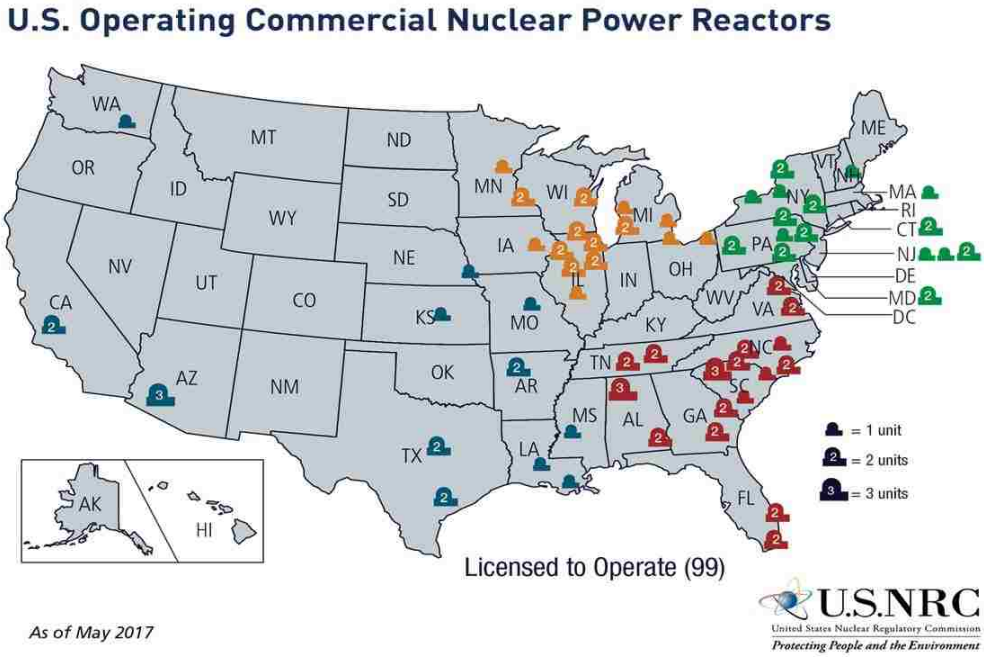

Figure 1.2. Map of nuclear power plants in the United States. Taken from U.S.NRC.

1.2. Radioanalytical Equipment

There is a variety of radioanalytical equipment capable of measuring the I-131 activity inside AgZ cartridges due to its beta particle and gamma ray emissions. The cartridges are usually taken to a low radiation background area (away from the plume) and measured (Maiello and Hoover, 2011). Both gamma-spectroscopy and Geiger-muller detectors may be used depending of the data quality objectives. If quantification is needed, γ-spectroscopy may be used due to higher counting and detection efficiencies. Geiger-muller detectors may be used qualitatively to determine if radionuclides are present or not. Two popular γ-spectroscopy detectors used are the portable sodium iodide activated with thallium (NaI (TI) scintillator) connected to a scaler and high-purity germanium (HPGe) (Maiello and Hoover, 2011). Though, due to ease of portability in the field, (The NaI (TI) scintillator will now be referred to as NaI probe for the rest of this paper) NaI probes are most often used. HPGe's require liquid nitrogen dewars for cooling the germanium crystal and would be too heavy to carry in the field, although have better energy resolutions. The NaI probe is connected to a scaler and the gross gamma emissions are counted in the field.

To use the NaI probe connected to a scalar, the detection system would have to be calibrated and a counting efficiency would have to be determined. Counting efficiency is radionuclide and source geometry dependent (Cember and Johnson, 2009). Meaning, that the same radionuclide would have to be measured and source geometry used during calibration to mimic the source in the field. If not, then a correction factor would have to be established. Due to the difficulties of using I-131 as a calibration standard, as mentioned earlier, Ba-133 is usually used as a surrogate due to its most abundant and energetic gamma energy being close in energy

to I-131's gamma. Counting efficiency is the ability for the detection equipment to register a count for every disintegration of an atom for the radionuclide measured. In mathematical terms:

$$\epsilon_{counting} = \frac{measured\ counts\ for\ radioisotope}{\#\ of disintegrations\ for\ radioisotope} \times 100\% = \%\ efficiency\ or\ \frac{counts}{disintegration}$$

Equation 1.1.

Counting efficiency is source geometry specific. To accurately determine the activity of a radionuclide, the counts measured by a detector would have to be divided by its counting efficiency or:

$$A\ (DPM) = \frac{Measured\ Counts\ (CPM)}{\epsilon_c \left(\frac{C}{D}\right)}$$

Equation 1.2.

A = activity in disintegrations per minute (DPM),

Measured counts = counts collected in a given time using a scalar,

ϵ_c = counting efficiency in counts per disintegration for the detector (CPD).

For this reason, source geometry must be carefully determined. As this is the same geometry that would be used in the field to determine the activity of a radioisotope.

Though, the approach of using a Ba-133 sealed point or planar source does not reflect the actual gaseous I-131 distribution inside the silver zeolite cartridge (Maiello and Hoover, 2011). As a result, there would be an underestimation in the measurement of gaseous I-131 activity in the plume (Maiello and Hoover, 2011). The underestimation in activity occurs from a larger solid angle emanating from the sealed point source used during calibration. Therefore, there are more photons collected by the detector. Though, in the field, the I-131 distribution is most likely to occur at a lower depth in the cartridge. This would result in a smaller solid angle emanating from the cartridge and less photons collected by the detector.

1.3. Silver Zeolite and Charcoal Cartridges

Silver zeolite cartridges have long been used for assaying radioiodine activity due to its ability to adsorb iodine while not adsorbing radioactive noble gases such as krypton-85 (Kr-85), xenon-133 (Xe-133) and xenon-135 (Xe-135) (Maiello and Hoover, 2011 and Cline, 1981). Radioactive noble gases mask the I-131 photopeaks and can saturate detectors. Silver zeolite has a strong preference for polar molecules and iodine is polar while noble gases are not. Silver zeolite works through an ion-exchange system (Maiello and Hoover, 2011).

Activated charcoal cartridges work through the process of chemisorption in that the radioiodines attach to a molecule called triethylenediamine (TEDA). Charcoal cartridges adsorb both radioiodine and noble gases. Therefore, during a nuclear incident, charcoal cartridges are usually not used (Maiello and Hoover, 2011).

Figure 1.3. Photograph of AgZ cartridge from F & J Specialty Products, INC. used in this project. Arrows

Figure 1.4. Photograph of an AgZ cartridge between two holders for a CAM. (Wang and Matthews, 2006).

1.4. Cylindrical (Face-loaded and Homogeneous) Geometries

Currently, there are two popular assumptions for the gaseous distribution of I-131 inside a charcoal cartridge after a sample has been taken in the field using an air sampler. These two assumptions are face-loaded distribution and homogeneous distribution. Literature reveals that the face-loaded distribution is the most widely accepted. Face-loaded distribution refers to the top 6.4 to 13 mm (.25 to 0.5") of the charcoal cartridge has adsorbed the I-131 (Montgomery, 1990). Therefore, if it is assumed that the I-131 is of the face-loaded distribution, then there would be an underestimate of the I-131 activity after a nuclear incident if the detector was calibrated using a single Ba-133 source. This is due to the gamma emissions are coming from a lower depth resulting in a smaller solid angle in the AgZ cartridge compared to coming off from above the cartridge.

The homogeneous distribution refers to all the charcoal inside the cartridge has adsorbed the I-131 evenly (Montgomery, 1990). If it is assumed that the I-131 is of the homogeneous distribution, then there would be an underestimate of the I-131 in the plume after a nuclear incident if the detector was calibrated using a single Ba-133 source. Again, this is due to gamma emissions coming from a lower depth resulting in a smaller solid angle in the charcoal cartridge compared to coming off from above the cartridge. Therefore, before using any radioanalytical equipment to measure the I-131 activity, the equipment needs to be properly calibrated to mimic the source geometry or distribution in the field. Also, the measurements done by Montgomery in 1990 were using charcoal cartridges. It is therefore assumed that an AgZ cartridge would perform by similar chemical and physical processes and have an exponential distribution (Maiello and Hoover, 2011).

1.5. Problem Statement

It is known that certain agencies may put a NaI probe on top of a single Ba-133 sealed point or planar source which would also be on top of an AgZ cartridge to calibrate their radioanalytical equipment; this would be no different than placing the point or planar source on the surface of a bench or table and placing the probe right on top of it. Therefore, underestimations in the calculated activity of I-131 would result in the field due to the higher counting efficiency for this geometry setup (i.e., the calibration source is closer to the detector and larger the solid angle). In the field, a face-loaded or homogeneous distribution of I-131 would most likely take place in the AgZ cartridge. For this reason, a conversion factor would be necessary to correct for the activity of I-131 calculated in the field. This would still allow the agency or institution to use a single Ba-133 point or planar source as a calibration standard. This study will compare various geometrical arrangements of both Ba-133 and I-131 fabricated spiked filter media in a silver zeolite cartridge to determine conversion factors that can be used to correct for the activity of I-131 measured in the field.

1.6. Objectives

This project will consist of three phases:

1. Phase I: Determine the effects of various geometries (i.e., above, inside-top, inside-middle, inside-bottom, and below) have on counting efficiencies for a Ba-133 point source placed in the vertical direction of a AgZ cartridge.
2. Phase II: Determine the effects of various geometries have on counting efficiencies for a planar and cylindrical (face-loaded and homogeneous) distribution inside an AgZ cartridge using liquid Ba-133 and filter papers.

3. Phase III: Determine the effects of various geometries have on counting efficiencies for a planar and cylindrical (face-loaded and homogeneous) distribution inside an AgZ cartridge using liquid I-131 and filter media.

With the counting efficiencies found in phases II and III, conversion factors can be calculated to correct for the I-131 activity measured in the field.

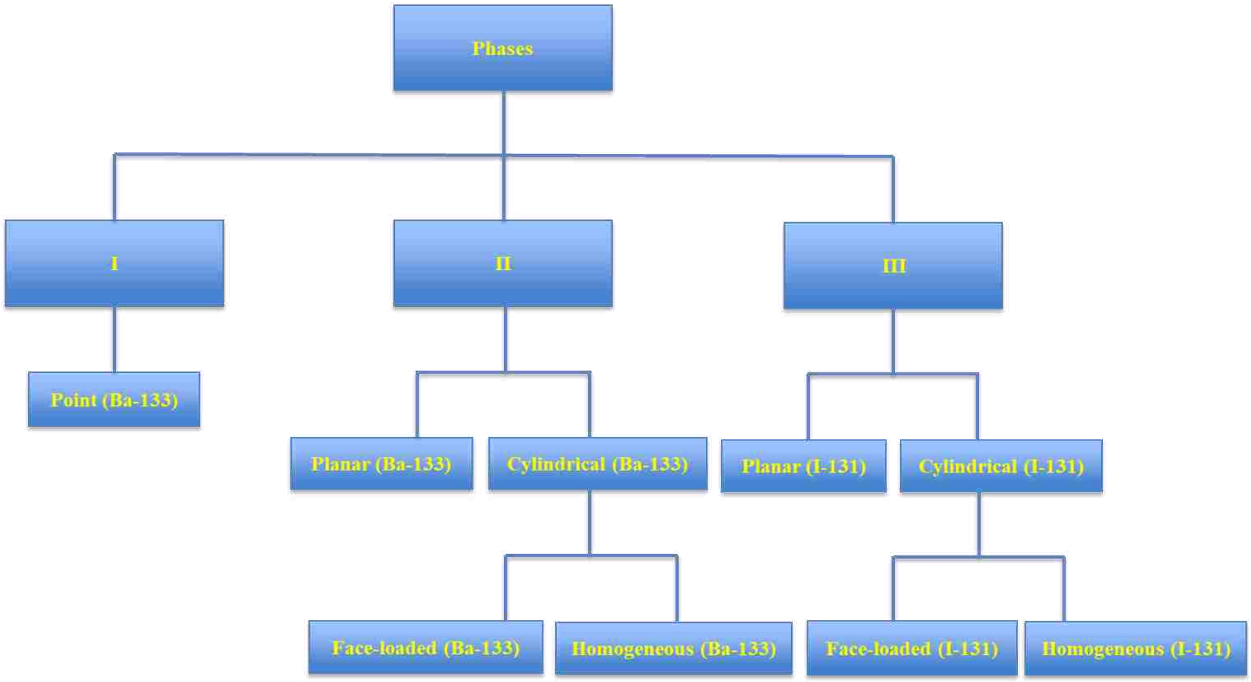

Figure 1.5. Chart showing the three phases of this project with its respective geometry and isotope.

CHAPTER 2. MATERIALS AND METHODS

2.1. Calibration of Scaler

2.1.1. Gamma-Detection System Specifications

To use the detection system for counting, the scaler (Ludlum Measurements, INC model 2000) that the NaI probe (Ludlum Measurements, INC model 44-10) was attached to had to be calibrated. This procedure was adopted by the calibration instructions included in the scalers product manual and done to ensure that the scaler was functioning properly and could register counts. The scaler was connected to a pulse generator or pulser (Ludlum Measurements, INC model 500). An operating voltage of 900 V was chosen for the detection system.

2.1.2. Verification of Counts Registered on Scaler

On the pulser, the multiplier dial was set to 1. The reading for the counts/minute (CPM) face on the pulser was then set to 40 counts/minute using the fine and coarse knobs. With the CPM face reading 40 CPM and the multiplier dial set to X1 this would correspond to a true value of 40 CPM on the pulser. Afterwards, the multiplier dial on the scaler was set to X1 and the minutes selector to 1. The “COUNT” button was then pressed on the scaler and began registering counts. These steps were then repeated for the X10, X100, and X1K on the pulser. The 400 CPM on the pulser was left alone and only the multiplier was changed. On the scaler, all counts for each multiplier on the pulser registered 400, 4,000, and 400,000 CPM respectively with a maximum error of 0.5%. Therefore, the verification of counts registered on the scaler was acceptable.

2.2. Ba-133 Sources in Different Positions in the Vertical Direction of an AgZ Cartridge (Phase I)

2.2.1. Characteristics of Silver Zeolite Cartridge

Before the Ba-133 point source could be placed inside the AgZ cartridge, the cartridge had to be opened. This was achieved by using a dremel tool. Once the seal to the cartridge was opened, the AgZ was weighed. The average weight for the AgZ was around 50 g. The AgZ cartridges used in this project came from F&J Specialty Products, INC. part # AGZC58 from LOT # 1305259-2. The dimensions of the cartridges are 5.74 ± 0.0254 cm (2.26 ± 0.01") in diameter and 2.67 ± 0.0254 cm (1.05 ± 0.01") in height. An AgZ mesh size of 50 x 80 was placed inside the cartridges. The cartridge housing is made of plastic. For different mesh sizes, there is an effect on the pressure drop inside the cartridges. The pressure will increase with decreasing mesh sizes (Gavilla, 2002 and Maiello and Hoover, 2011). Typically, AgZ cartridges are offered as 16 x 40, 30 x 50, and 50 x 80 mesh sizes. Therefore, the 50 x 80 mesh size is the mostly widely used AgZ used and chosen for this project.

Figure 2.1. Components of an AgZ cartridge. From left to right: lid, filter paper, canister, and second filter paper.

2.2.2. Specifications for the Ba-133 Point Source

The activity chosen for the Ba-133 point source was 3.7 kBq or 0.1 µCi. This activity is typically used for calibrating gamma-spectroscopy systems. The source was obtained from

Spectrum Techniques, LLC. According to the manufacturer, the dimensions for the source is 2.54 cm (1") in diameter and 0.318 cm (0.125") in height.

2.2.3. Placement of Source inside the AgZ Cartridge and Counting

Five 2-minute background counts were counted with a blank cartridge placed under the probe and then averaged and normalized to CPM. Placement of the Ba-133 point source inside the AgZ cartridge was done by removing the front cover and filter paper. The source was placed on the top face of the cartridge with the sensitive surface facing up. The filter paper and cover were then placed on top of the source. The cartridge was then pressed down to mimic its original dimensions and sealed using electric tape. The following source position or geometries were then counted using the AgZ cartridge: above, inside-top, inside-middle, inside-bottom, and below. Each source position was counted independently of the other and placed at the centerline of the probe. Five 5-minute counts were counted per source position and then averaged and normalized to CPM. A net CPM was then calculated by subtracting the background counts from the source counts, and the result recorded in CPM as well as the counting efficiency.

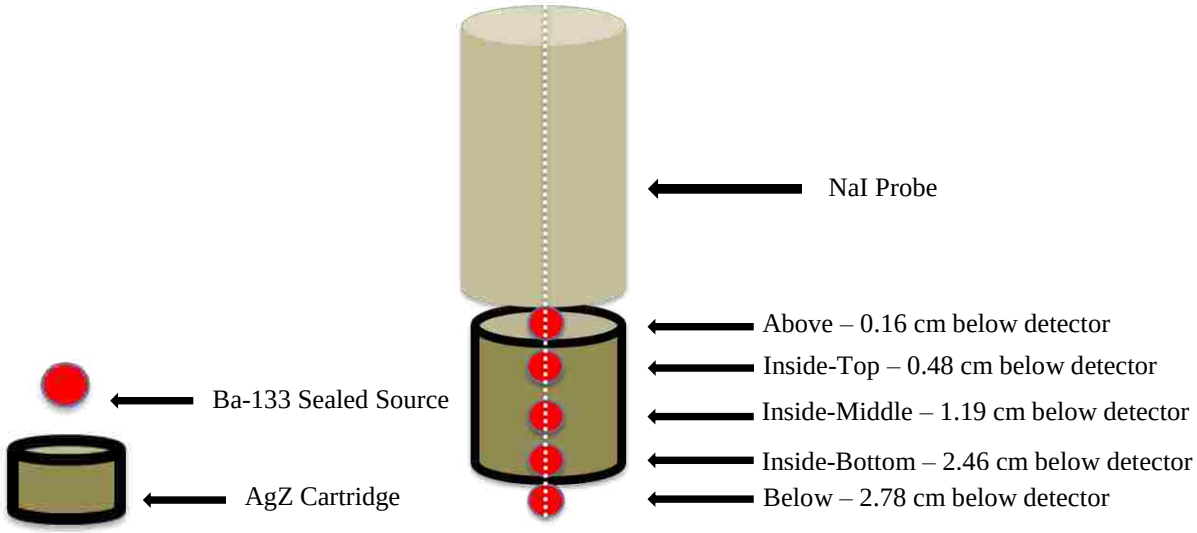

Figure 2.2. Schematic of NaI probe placed on top of the AgZ cartridge. The Ba-133 source was placed in 5 different positions along the vertical centerline of the cartridge and counted independently of the other.

2.3. Sources in Different Geometries using Liquid Ba-133 in the Vertical Direction of an AgZ Cartridge (Phase II)

2.3.1. Properties of filters and liquid Ba-133

In addition to the Ba-133 point source, other geometries were prepared using filter papers (Whatman Qualitative Grade 4) with a pore size of 20-25 µm. This filter paper grade was chosen due to its large pore size and retention of liquid without leaking. The other geometries prepared using liquid Ba-133 are planar and cylindrical. The cylindrical geometry was split into two sub geometries: face-loaded and homgeneous. The liquid Ba-133 used was produced by Eckert and Ziegler. The activity ordered was 185 kBq (5 µCi) in 5 ml $BaCl_2$ solution. The Ba-133 solution is NIST traceable from the manufacturer. For a laboratory to meet the criteria for NIST traceable, it must be fully equipped to calibrate equipment or solutions to the National Institute of Standards and Technology (NIST) standards. Also, any products that are produced by the laboratory would have to match the NIST-maintained measurement standards. NIST is a non-regulatory federal agency who develops measurement, standards, and technologies to improve production (Sargis, 2018).

2.3.2. Preparation of Planar Geometry and Counting

To prepare the filters for the planar geometry, the filter paper was cut into a 5.08 cm (2") diameter circle. The liquid Ba-133 was diluted to 3.7 kBq (0.1 µCi) and blue dye was added for visualization of the solution. The methodology used to prepare the filter papers was adopted by Wang and Matthews to mimic gaseous I-131 using liquid I-131 (Wang and Matthews, 2006). Before pipetting the solution, the filter paper was placed on top of saran wrap and then placed into a petri dish. This was done to trap any leakage of the radioactive solution. Twelve 50 µl drops of liquid Ba-133 were pipetted onto the filter paper in a checkerboard pattern (figure 2-3). For the planar geometry, only one filter paper was used, and a total of 600 µl was pipetted onto

the filter paper. The 600 µl was equivalent to 3.7 kBq (0.1 µCi) Ba-133. After pipetting the solution onto the filter paper, the filter paper was dried for ~24 hours. Once dried, the filter paper was placed on top of an AgZ cartridge with saran wrap covering both faces of the paper.

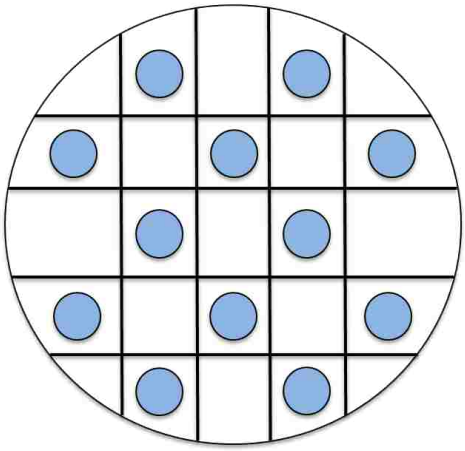

Figure 2.3. Schematic of drops pipetted on to a filter paper with a checkerboard pattern.

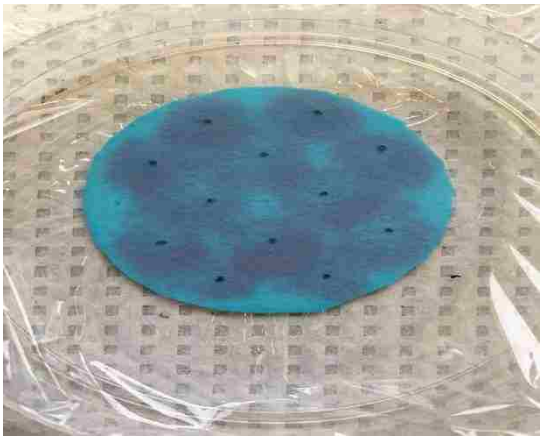

Figure 2.4. Filter paper with liquid Ba-133 solution right after pipetting.

Figure 2.5. Filter paper with liquid Ba-133 solution after 24 hours.

Before counting the spiked filter, a filter with $NaCl_2$ was made as a blank. Five 2-minute background counts were counted using the blank and averaged together and normalized to CPM. Afterwards, five 5-minute counts were counted using the spiked filter paper and averaged together and normalized to CPM. A net CPM was then calculated by subtracting the background counts from the source counts, and the result recorded in CPM. This was repeated two more

times for two additional spiked filters for a total of three replicates. All filter papers were placed on top of the cartridge in the middle and placed at the centerline of the probe.

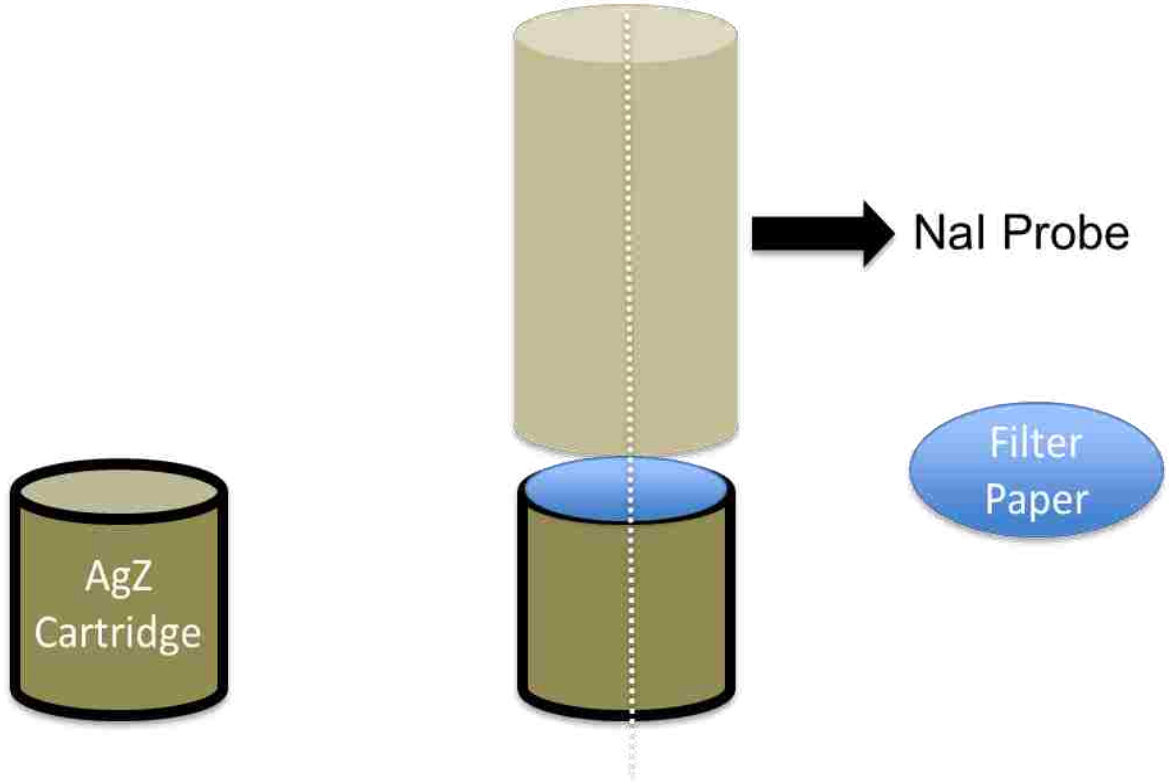

Figure 2.6. Planar filter paper on top of an AgZ cartridge.

2.3.3. Preparation of Face-Loaded Geometry and Counting

To prepare the filter papers for the face-loaded geometry, the filter paper was cut into a 5.04 cm (2") diameter circle. The liquid Ba-133 was diluted to 3.7 kBq (0.1 µCi) and blue dye was added for visualization of the solution. The solution was then pipetted onto the filter paper in a checkerboard pattern. The methodology used to prepare the filter papers was the same as that for the planar geometry. Before pipetting the solution, the filter paper was placed on top of saran wrap and then placed into a petri dish. This was done to trap any potential leakage of the radioactive solution. Twelve 50 µl drops of liquid Ba-133 were pipetted onto the filter paper. For the face-loaded geometry, three filter papers were used, and a total of 1,800 µl was pipetted onto

the set of filter papers (600 µl per filter paper). The 1,800 µl was equivalent to 3.7 kBq (0.1 µCi) Ba-133. After pipetting the solution onto the filter papers, they dried for ~24 hours. Once dried, the filter papers were ready to be placed inside an AgZ cartridge. The cartridge was opened using a dremel tool. The AgZ was removed and weighed. Three even layers of AgZ (around 7.3 g per layer) were prepared with each layer separated by a spiked filter. Each layer equated to 0.34 cm (0.135"). The remaining AgZ was placed under the third filter which was around 22 g and

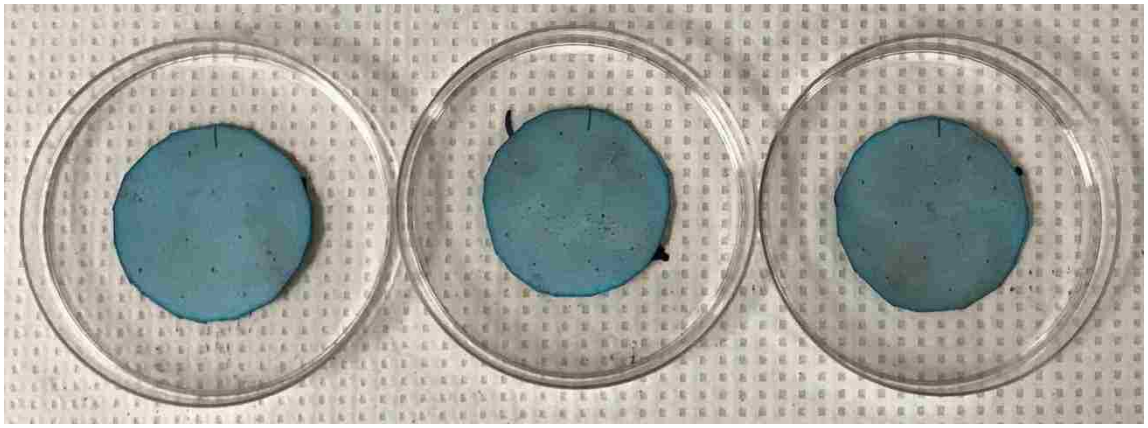

Figure 2.7. Three filter papers for face-loaded geometry.

equated to 1.03 cm (0.405"). Each spiked filter paper was rotated 90º to prevent asymmetries (Wang and Matthews, 2006). The filter paper (for the cartridge itself) and cover were then placed on top of the final layer of AgZ. The cartridge was then pressed down to mimic its original dimensions and sealed using electric tape.

Before counting the spiked filters, a filter with $NaCl_2$ was made as a blank. Five 2-minute background counts were counted using the blank and averaged together and normalized to CPM. Afterwards, five 5-minute counts were counted using the spiked filter paper and averaged together and normalized to CPM. A net CPM was then calculated by subtracting the background counts from the source counts, and the result recorded in CPM. This was repeated two more times for six additional spiked filters for a total of three replicates. All filter papers were placed

in the middle of the cartridge and placed at the centerline of the probe. The probe was placed directly on top of the cartridge for all measurements.

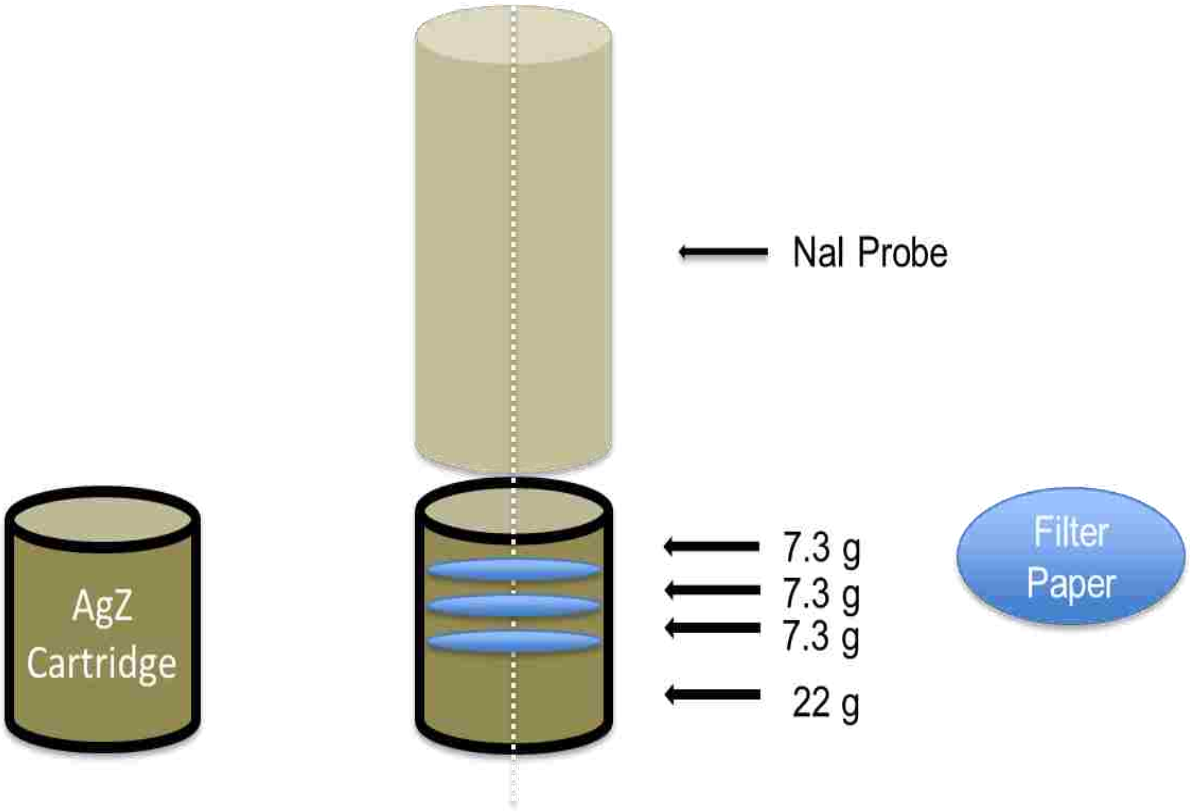

Figure 2.8. Three filter papers inside an AgZ cartridge mimicking face-loaded geometry.

2.3.4. Preparation of Homogeneous Geometry and Counting

To prepare the filters for the homogeneous geometry, the filter paper was cut into 5.04 cm (2") diameter circle. The liquid Ba-133 was diluted to 3.7 kBq (0.1 µCi) and blue dye was added for visualization of the solution. The solution was then pipetted onto the filter paper in a checkerboard pattern. The methodology used to prepare the filter papers was the same as for the planar geometry. Before pipetting the solution, the filter paper was placed on top of saran wrap and then placed into a petri dish. This was done to trap any leakage of the radioactive solution. Twelve 50 µl drops of liquid Ba-133 were pipetted onto the filter paper. For the homogeneous geometry, five filter papers were used, and a total of 3,000 µl was pipetted onto the set of filter

papers (600 µl per filter paper). The 3,000 µl was equivalent to 3.7 kBq (0.1 µCi) Ba-133. After pipetting the solution onto the filter papers, they dried for ~24 hours. Once dried, the filter papers were ready to be placed inside an AgZ cartridge. The method for placing the filter papers inside the AgZ cartridge was the same as that for the point source. The cartridge was opened using a dremel tool. The AgZ was removed and weighed. Six even layers of AgZ were prepared with each layer separated by a spiked filter. Each layer equated to 0.34 cm (0.135"). Again, each spiked filter paper was rotated 90º to prevent asymmetries. The filter paper (for the AgZ

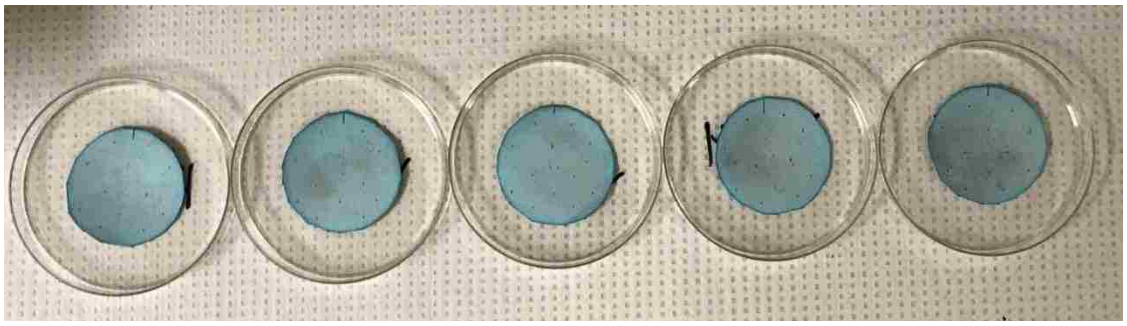

Figure 2.9. Five filter papers for face-loaded geometry.

cartridge) and cover were then placed on top of the final layer of AgZ. The cartridge was then pressed down to mimic its original dimensions and sealed using electric tape.

Before counting the spiked filters, a filter with $NaCl_2$ was made as a blank. Five 2-minute background counts were counted using the blank and averaged together and normalized to CPM. Afterwards, five 5-minute counts were counted using the spiked filter paper and averaged together and normalized to CPM. A net CPM was then calculated by subtracting the background counts from the source counts, and the result recorded in CPM. This was repeated two more times for ten additional spiked filters for a total of three replicates. All filter papers were placed in the middle of the cartridge and placed at the centerline of the probe. The probe was placed directly on top of the cartridge for all measurements.

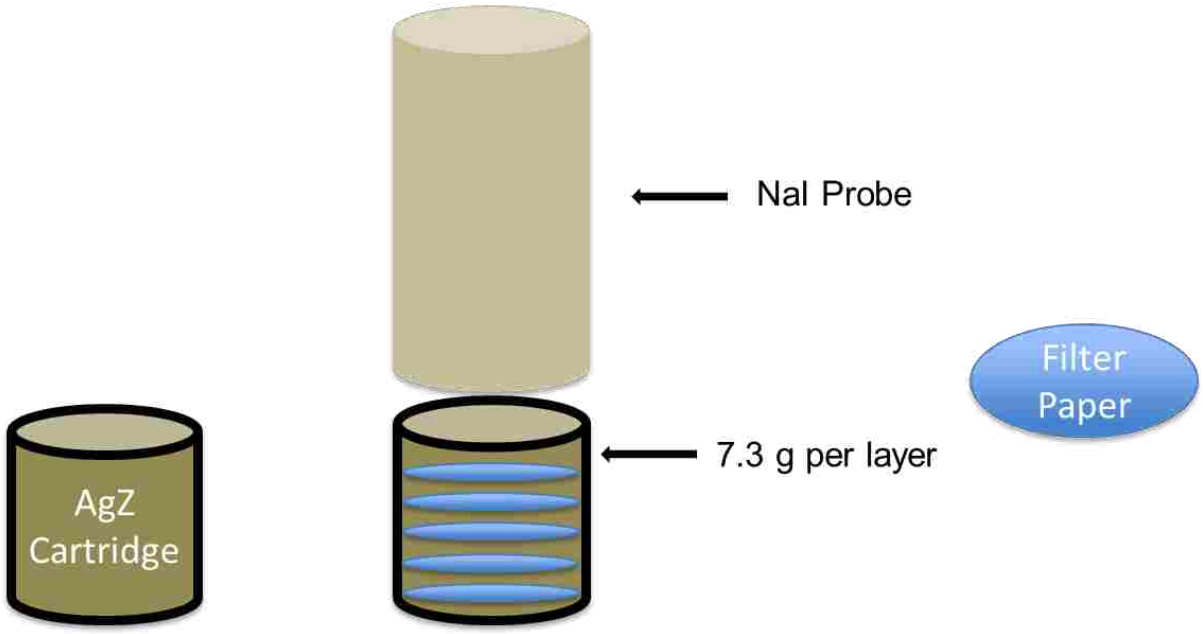

Figure 2.10. Five filter papers inside an AgZ cartridge mimicking homogeneous geometry.

2.4. Sources in Different Geometries using Liquid I-131 in the Vertical Direction of an AgZ Cartridge (Phase III)

Like the preparation of the planar, face-loaded, and homogeneous geometries using liquid Ba-133, the liquid I-131 had to be diluted and pipetted onto the filter papers. The liquid I-131 was ordered from Cardinal Health (a local radiopharmaceutical company in Baton Rouge, Louisiana). The activity ordered was 37 Mbq (1 mCi) in 1 ml distilled water. The radioisotope was carrier free and the activity used was that calibrated by the company.

The same procedures for preparation of the filter papers using liquid Ba-133 were followed to prepare the I-131 spiked filter papers. All iodinations were done in an approved hood for use of radioisotopes with the proper flow rate. Once the filter papers dried for ~24 hours, they were placed inside the cartridges for each respective geometry and counted. Due to the 8.02-day half-life of I-131, the activity and therefore counts had to be decay corrected back to the original calibration date and time done by the company. To simulate the point source geometry for I-131, a blank point source with the same dimensions of that of the Ba-133 point source was used. The

solution of liquid I-131 was diluted to 50 µl to equal an activity of 3.7 kBq (0.1 mCi). The diluted solution was then pipetted on to the middle of the blank point source and a piece of tape placed over it.

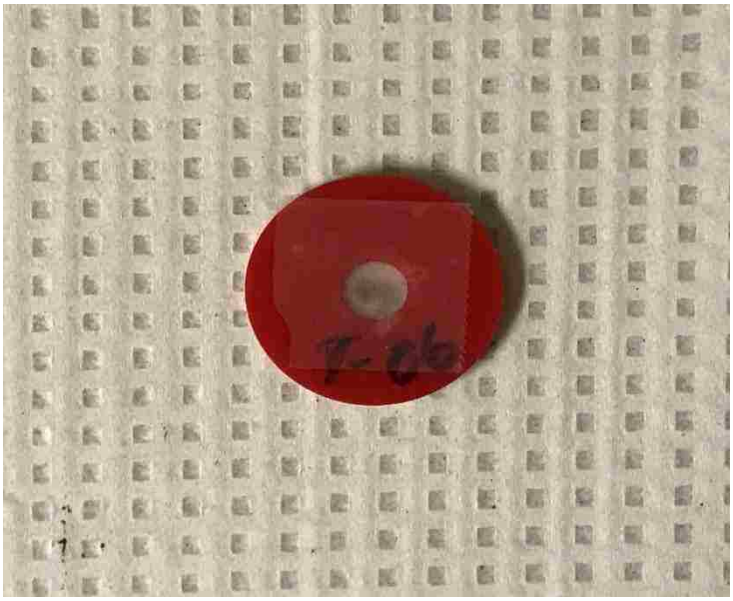

Figure 2.11. Fabricated 0.1 µCi I-131 point source.

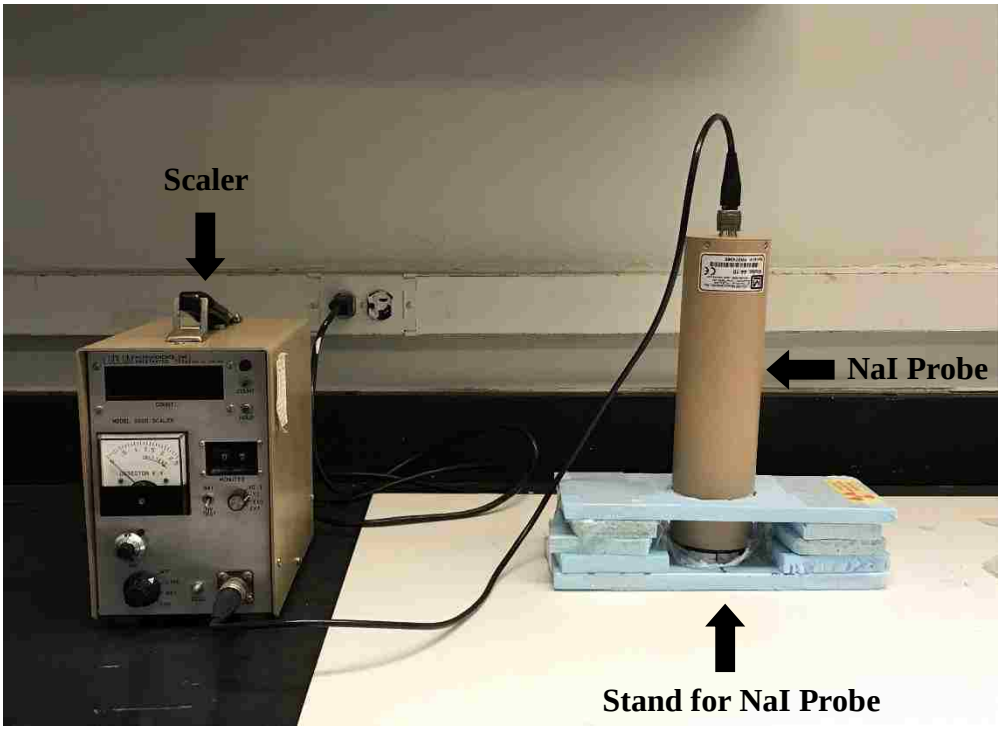

Figure 2.12. Setup of NaI Detection system used to count AgZ cartridges. The NaI probe, sources (point and filter papers), and AgZ cartridge were all at centerline in the vertical position.

2.5. Radiation Safety Concerns (ALARA)

In order to maintain the ALARA philosophy (As Low As Reasonably Achievable), radiation protection standards had to be taken into consideration. Time, distance, and shielding was the major precautions taken into place. Preparation of the filters with both Ba-133 and I-131 were done behind a plexiglass shield lined with lead bricks surrounding the area. Lab coat and gloves were used. Also, all areas where radioactive material was used were surveyed for any potential contamination along with hands and feet.

CHAPTER 3. RESULTS AND DISCUSSION

3.1. Consistency of Spiked Filter Papers

3.1.1. Filter Comparisons per Geometry

To determine that the filter papers for each geometry were spiked consistently, each filter paper was counted independent of the other and compared. This was done by placing saran wrap around the filter paper (to prevent contamination of the probe) and placing it on top of a non-spiked AgZ cartridge in the middle. The NaI probe was then placed on top of the filter paper and positioned at the centerline of the cartridge.

Prior to counting, five 1-minute background counts were taken using the $NaCl_2$ blank and averaged. Five 1-minute counts were then taken using the spiked filters and averaged. The net CPM was then calculated and compared for each filter paper and its respective geometry. A total of 27 filters were counted: 3 for the planar geometry, 9 for the face-loaded geometry, and 15 homogeneous geometry. No statistical differences were found at the 95% confidence level among the filters for their respective geometries. This concludes that the filters papers were spiked consistently.

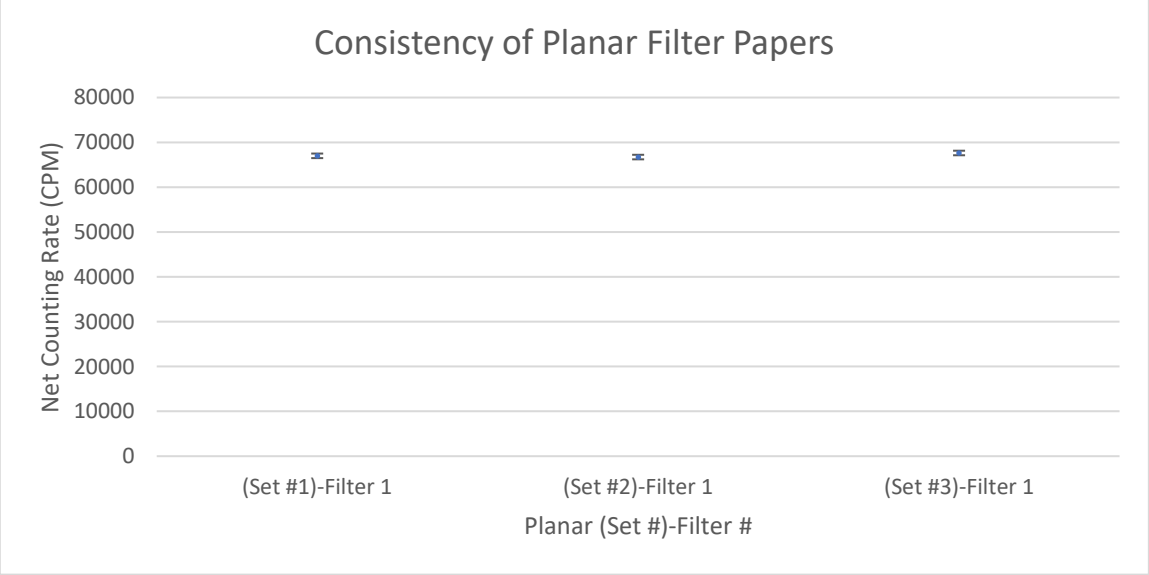

Figure 3.1. Plot of net counting rate (CPM) versus filter paper # for planar geometry.

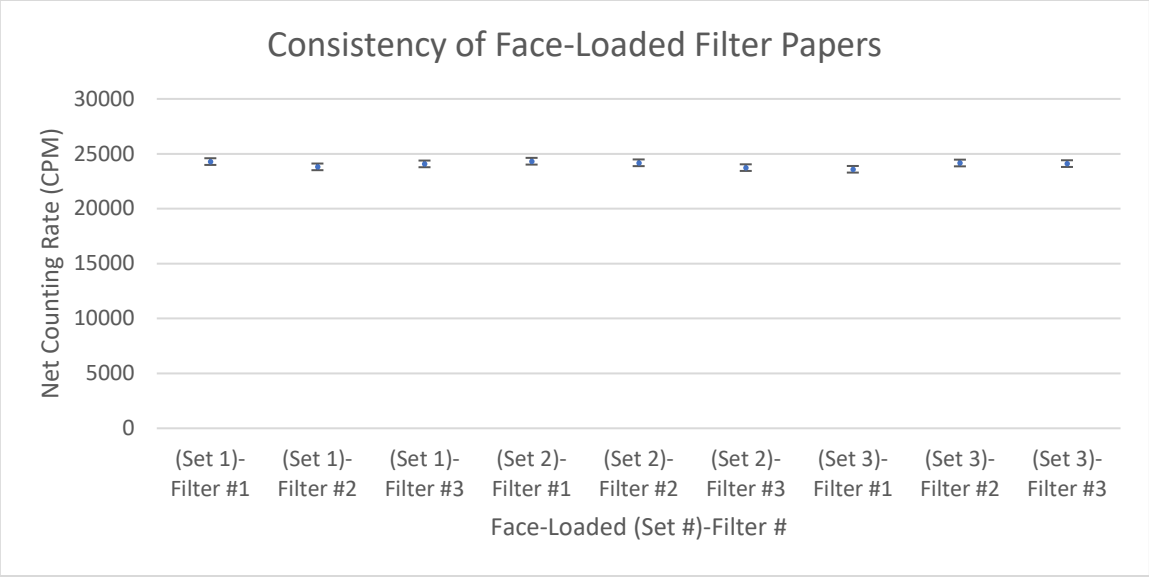

Figure 3.2. Plot of net counting rate (CPM) versus filter paper # for face-loaded geometry.

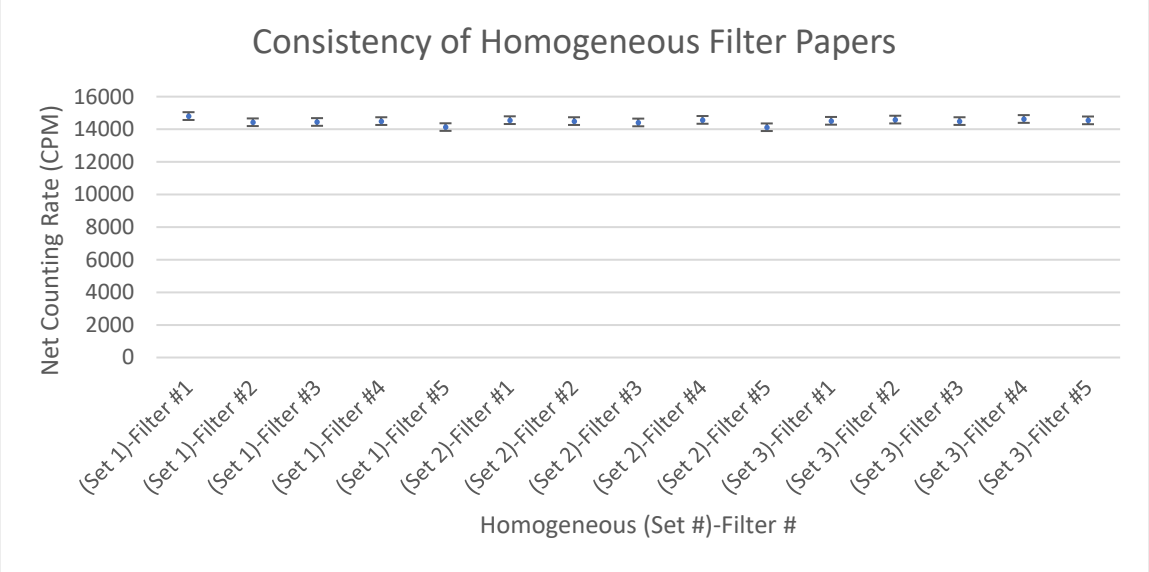

Figure 3.3. Plot of net counting rate (CPM) versus filter paper # for homogeneous geometry.

3.1.2. Homogeneity of Spiked Filter Papers

The homogeneity of the liquid Ba-133 needed to be tested to ensure an even spread on the filter papers. This will provide evidence that the radioactivity of the radioisotope was consistent around the area of the filter papers. Two methods were used:

1. Using a High Purity Germanium (HPGe) detector and,

2. Using a collimated 1" thick lead brick

The first method involved destructive testing. A filter paper with planar geometry was made (as in section 2.3.2) and cut into 4 even quadrants. Each quadrant was placed inside a HPGe detector at the center and counted for two minutes each. The area of the 356 keV photopeak for Ba-133 was then analyzed. According to the counts measured, there were no statistical differences among the quadrants at the 95% confidence level (figure 3-5). This concludes that each quadrant of the filter paper contained approximately the same amount of radioactivity.

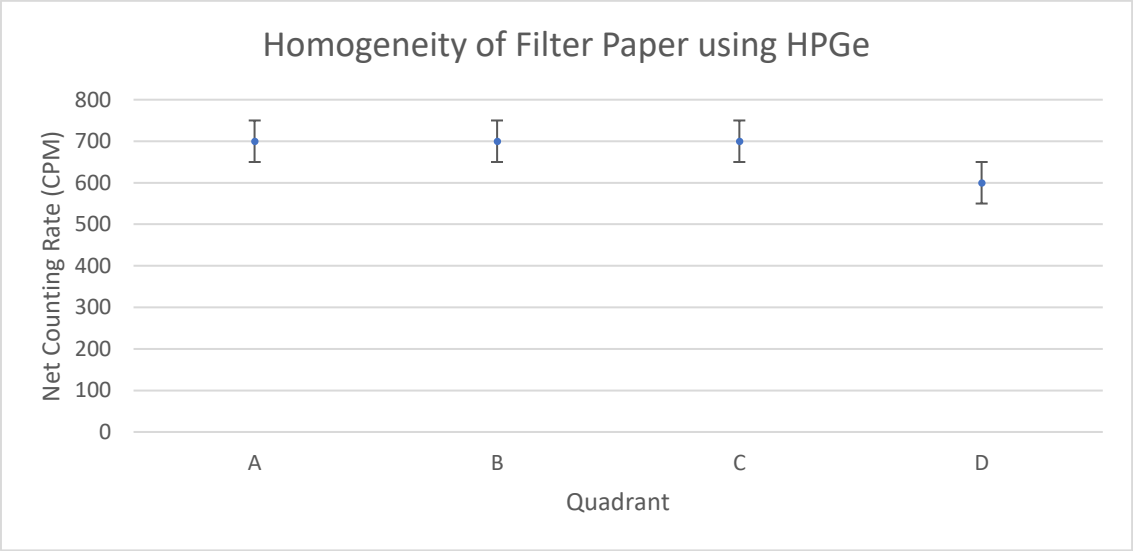

Figure 3.4. Plot of net counting rate (CPM) versus quadrant of a filter paper in the planar geometry counted using an HPGe detector.

The second method involved non-destructive testing. A 0.5" hole was drilled into a 1"thick lead brick. One of the filter papers with planar geometry made previously (as in section 2.3.2) was placed on top of a silver zeolite cartridge at the center. The filter paper was divided into 4 quadrants but without cutting them apart. A line 45º from the center of the filter paper was drawn for each quadrant. A dot 0.5" in diameter was then drawn at the middle of each line of the quadrant. The filter paper was then placed on top of an AgZ cartridge. The collimated lead brick was then placed on one quadrant. The brick was centered so that the hole was aligned with the

dot on the filter paper. The NaI probe was then placed on top of the hole of the brick at the centerline. A 2-minute count was then taken. The above steps were repeated for each quadrant and at the center of the filter paper. The counts were normalized to CPM. According to the counts measured, there were no statistical differences at the 95% confidence interval among each quadrant and at the center of the filter paper (figure 3-6). This concludes that each quadrant of the filter paper contained approximately the same amount of radioactivity.

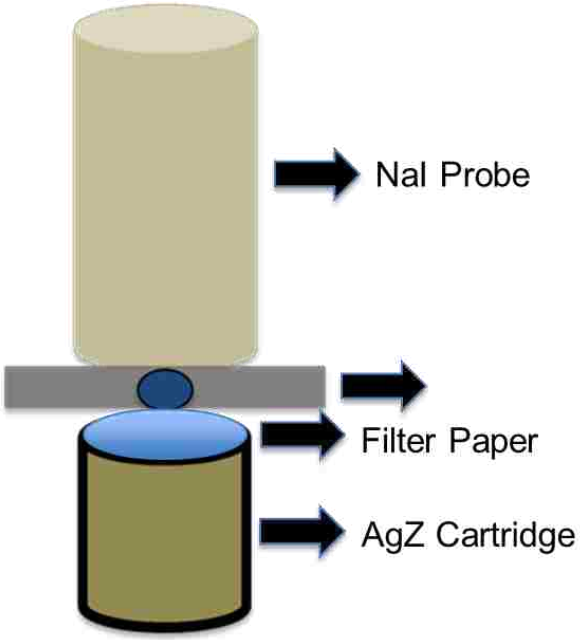

Figure 3.5. Schematic of collimated lead brick on top of spiked filter paper and AgZ cartridge.

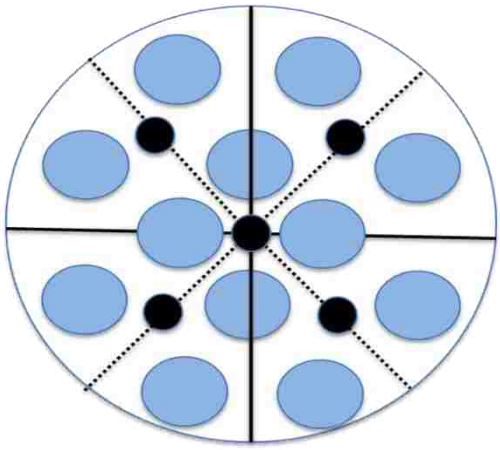

Figure 3.6. Schematic of top view of filter paper used with collimated lead brick. Dots were placed at the center of the 45° line from the middle of the filter paper.

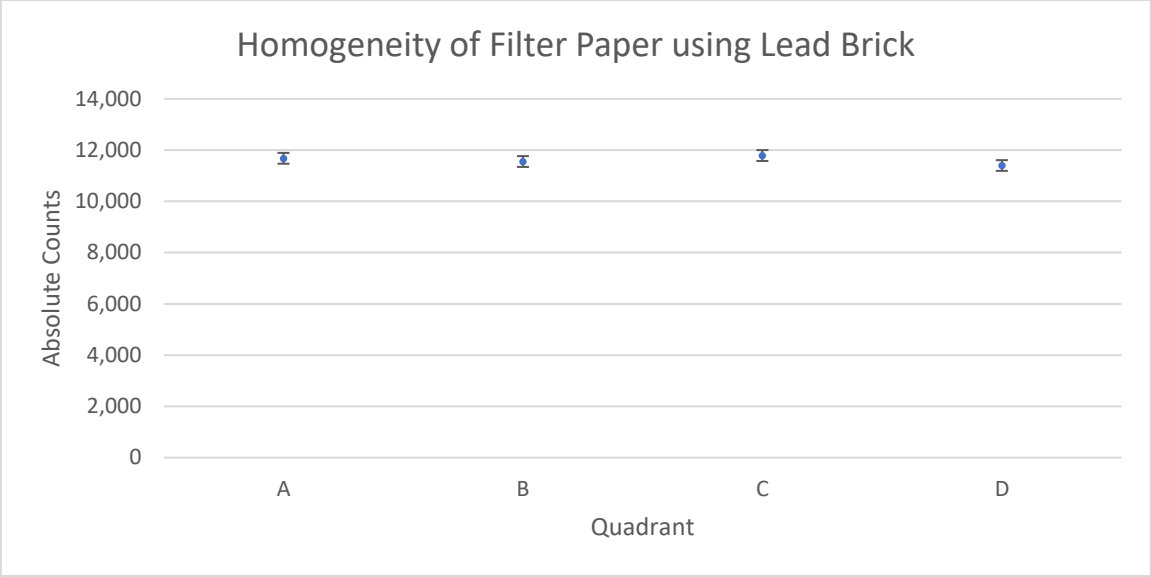

Figure 3.7. Plot of absolute counts versus quadrant of a filter paper in the planar geometry. A collimated lead brick was used to show homogeneity of radioactivity throughout the filter paper.

3.2. Phase I (Ba-133 Point Source Geometry)

A single 0.1 µCi Ba-133 point source was used in phase 1 to determine the effects on the net counting rate and counting efficiency of an NaI probe by increasing the distance of the source from the probe. Five different locations were tested in the AgZ cartridge: above, inside-top, inside-middle, inside-bottom, and below. As expected, the larger the distance of the source from the probe, the lower the net counting rate and counting efficiency. Also, when the source was placed inside the AgZ cartridge, attenuation of the photons had an effect. There were significant differences of both the net counting rate and counting efficiencies at the 95% confidence level between the different positions. There was a 40% decrease in the net counting rate between the source placed above the cartridge and the source placed inside the middle of the cartridge (146,000 ± 400 CPM for above position and 58,800 ± 200 CPM for inside-middle position). The inside-middle position is critical because this would resemble a face-loaded geometry in the field. In effect, an underestimation of the activity of I-131 would occur and therefore the calculated dose equivalents using the algorithms.

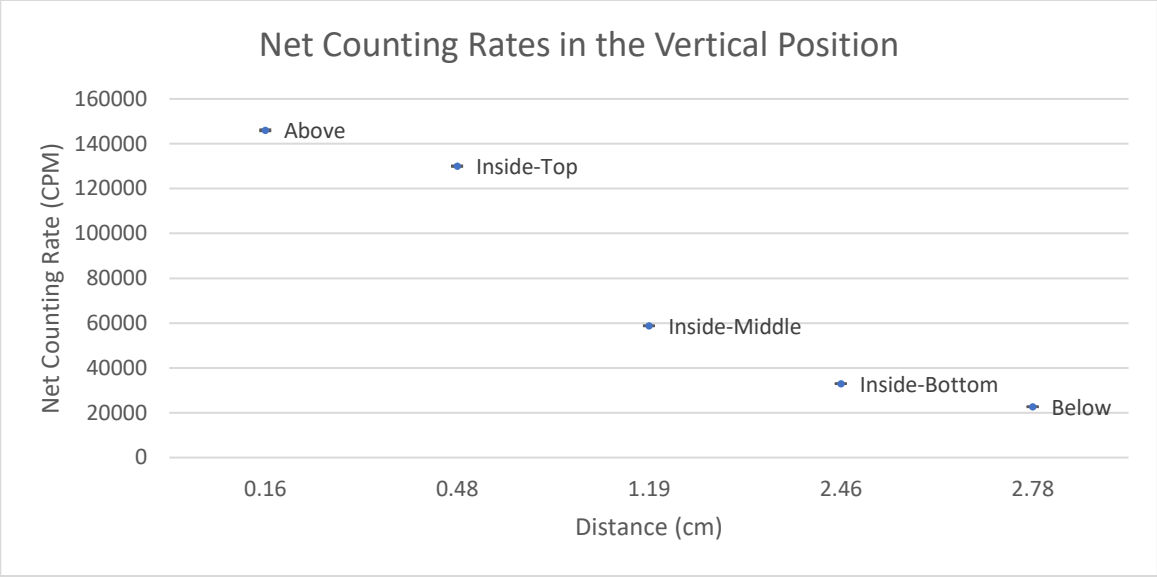

Figure 3.8. Plot showing the net counting rate versus distance of Ba-133 point source in AgZ cartridge from detector face.

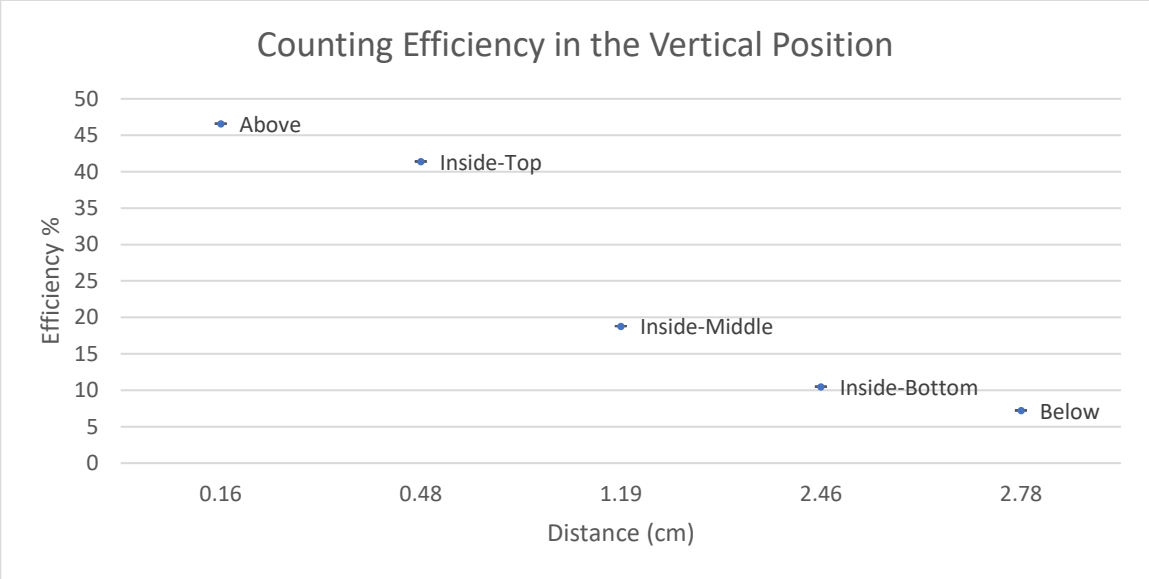

Figure 3.9. Plot showing the counting efficiency versus distance of Ba-133 point source in AgZ cartridge from detector face.

3.3. Phase II (Ba-133, Planar, Face-Loaded, and Homogeneous Geometries)

3.3.1. Planar Source Geometry

The filter paper with planar source geometry was placed on top of the AgZ cartridge for counting. There were no statistical differences at the 95% confidence level among the three replicates in both the net counting rate and counting efficiency. The net counting rate averaged

among the three replicates was 67,100 ± 300 CPM, while the counting efficiency averaged among the three replicates was 31 ± 0.016%. Comparing this geometry to a point source geometry, the net counting rate decreased by 53% (142,500 ± 400 CPM versus 67,100 ± 300 CPM). The counting efficiency of the detection system also decreased by 16 percentage points.

3.3.2. Face-Loaded Geometry

Three filter papers mimicking face-loaded geometry were placed inside of the AgZ cartridge for counting. There were no statistical differences at the 95% confidence among the three replicates in both the net counting rate and counting efficiency. The net counting rate averaged among the three replicates was 29,700 ± 200 CPM, while the counting efficiency averaged among the three replicates was 14 ± 0.0071%. Comparing this geometry to a point source geometry, the net counting rate decreased by 80% (142,500 ± 400 CPM versus 29,700 ± 200 CPM). The counting efficiency of the detection system also decreased by 33 percentage points.

3.3.3. Homogeneous Geometry

Five filter papers mimicking homogeneous geometry were placed inside of the AgZ cartridge for counting. There were no statistical differences at the 95% confidence level among the three replicates in both the net counting rate and counting efficiency. The net counting rate averaged among the three replicates was 27,200 ± 200 CPM, while the counting efficiency averaged among the three replicates was 13 ± 0.0066%. Comparing this geometry to a point source geometry, the net counting rate decreased by 81% (142,500 ± 400 CPM versus 27,200 ± 200 CPM). The counting efficiency of the detection system also decreased by 34 percentage points. The differences in both net counting rate and counting efficiency for both face-loaded and homogeneous geometries were less than 5%. From this data, the conclusion is that the photons

being emitted from the bottom two filter papers inside the AgZ cartridge are attenuated before reaching the probe.

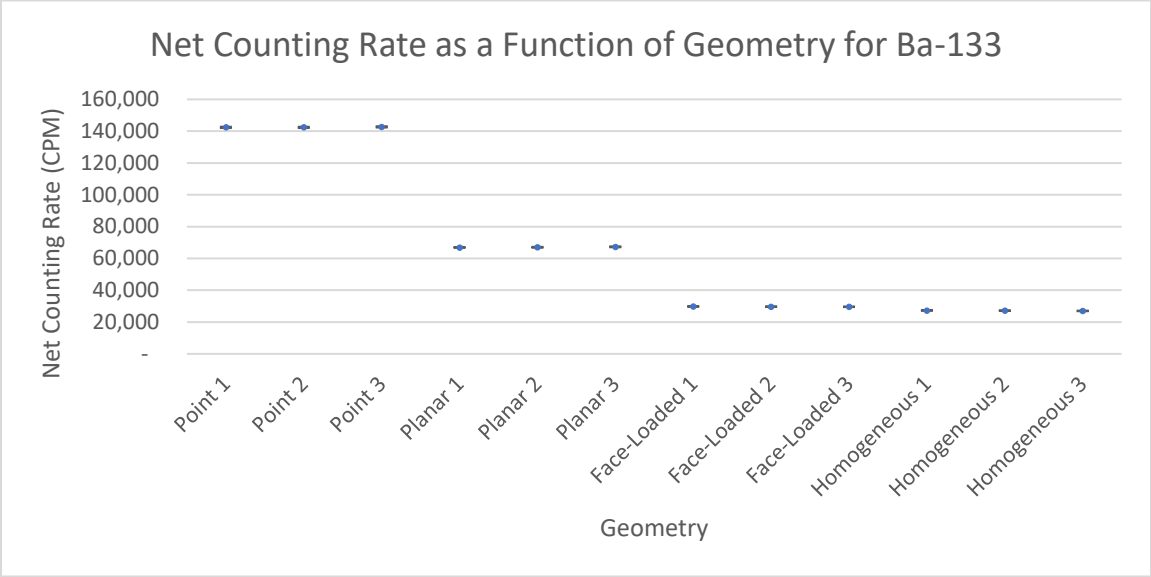

Figure 3.10. Plot showing the net counting rate (CPM) versus geometry per replicate.

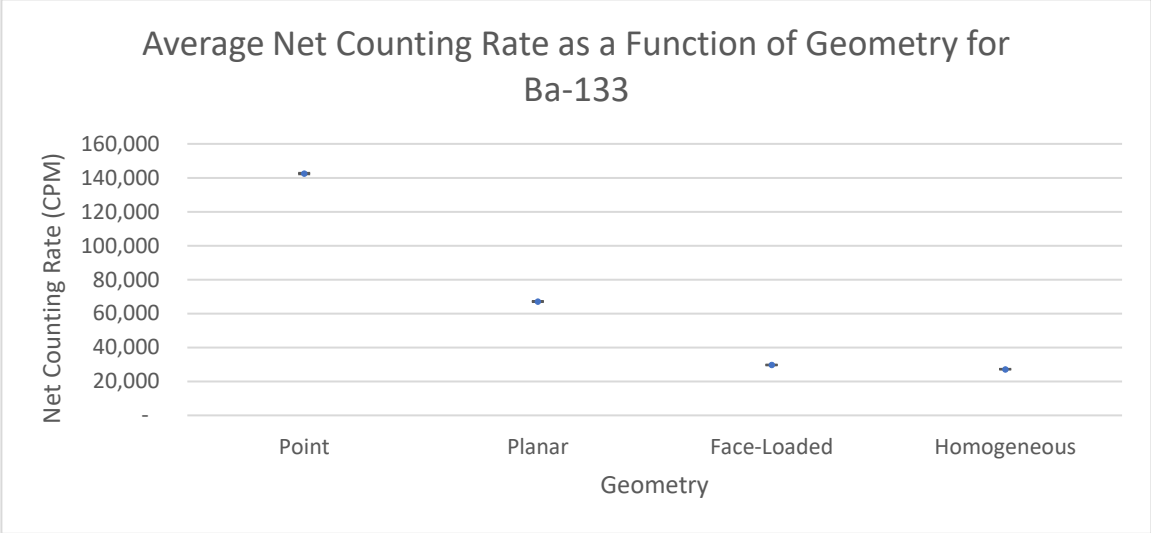

Figure 3.11. Plot showing the average net counting rate (CPM) versus geometry.

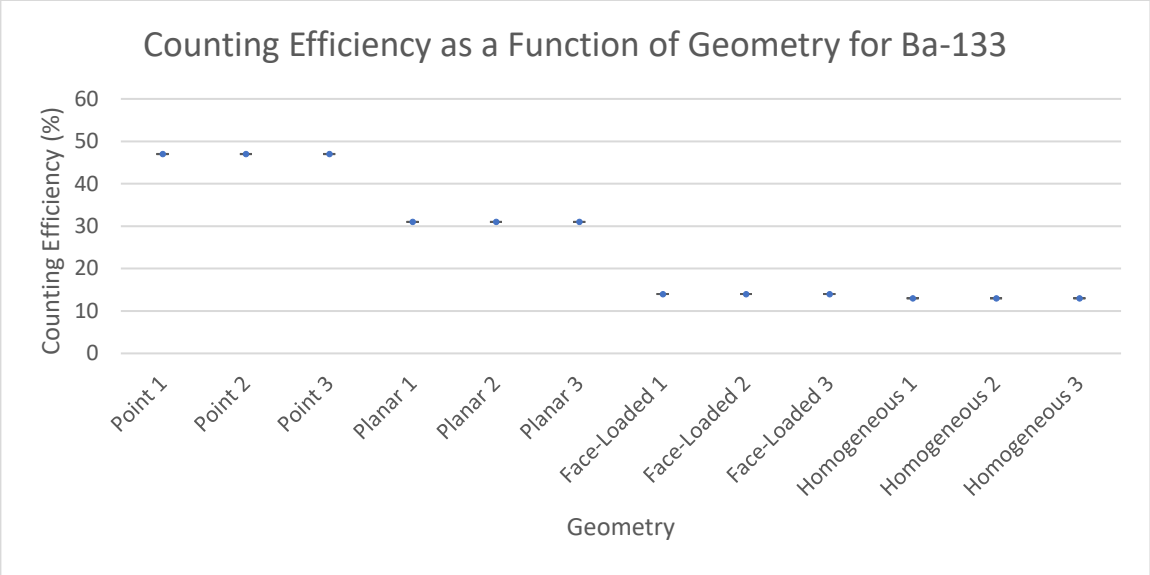

Figure 3.12. Plot showing the counting efficiency (%) versus geometry per replicate.

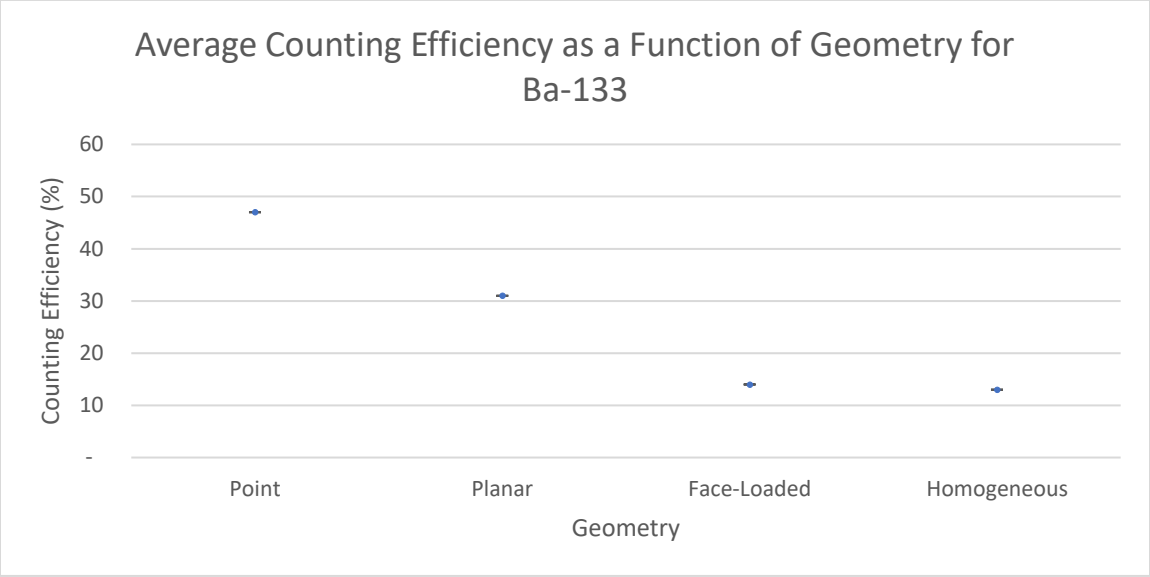

Figure 3.13. Plot showing the average counting efficiency (%) versus geometry.

3.4. Phase III (I-131, Planar, Face-Loaded, and Homogeneous Geometries)

3.4.1. Point Source Geometry

The point source geometry with liquid I-131 was placed on top of the AgZ cartridge for counting. There were no statistical differences at the 95% confidence level among the three replicates in both the net counting rate and counting efficiency. The net counting rate averaged

among the three replicates was 34,600 ± 200 CPM, while the counting efficiency averaged among the three replicates was 16 ± 0.0081%.

3.4.2. Planar Source Geometry

The filter paper with planar source geometry was placed on top of the AgZ cartridge for counting. There were no statistical differences at the 95% confidence level among the three replicates in both the net counting rate and counting efficiency. The net counting rate averaged among the three replicates was 22,200 ± 200 CPM, while the counting efficiency averaged among the three replicates was 10 ± 0.0051%. Comparing this geometry to a point source geometry, the net counting rate decreased by 36% (34,600 ± 200 CPM versus 22,200 ± 200 CPM). The counting efficiency of the detection system also decreased by 6 percentage points.

3.4.3. Face-Loaded Geometry

Three filter papers mimicking face-loaded geometry were placed inside of the AgZ cartridge for counting. There were no statistical differences at the 95% confidence among the three replicates in both the net counting rate and counting efficiency. The net counting rate averaged among the three replicates was 12,000 ± 200 CPM, while the counting efficiency averaged among the three replicates was 6 ± 0.003%. Comparing this geometry to a point source geometry, the net counting rate decreased by 65% (34,600 ± 200 CPM versus 12,000 ± 200 CPM). The counting efficiency of the detection system also decreased by 10 percentage points.

3.4.4. Homogeneous Geometry

Five filter papers mimicking homogeneous geometry were placed inside of the AgZ cartridge for counting. There were no statistical differences at the 95% confidence level among the three replicates in both the net counting rate and counting efficiency. The net counting rate averaged among the three replicates was 10,000 ± 200 CPM, while the counting efficiency

averaged among the three replicates was 5 ± 0.003%. Comparing this geometry to a point source geometry, the net counting rate decreased by 71% (34,600 ± 200 CPM versus 10,000 ± 200 CPM). The counting efficiency of the detection system also decreased by 11 percentage points. It is seen that the differences in both net counting rate and counting efficiency for both face-loaded and homogeneous geometries were less than 11%. From this data, the conclusion is that the photons being emitted from the bottom two filter papers inside the AgZ cartridge are attenuated before reaching the probe.

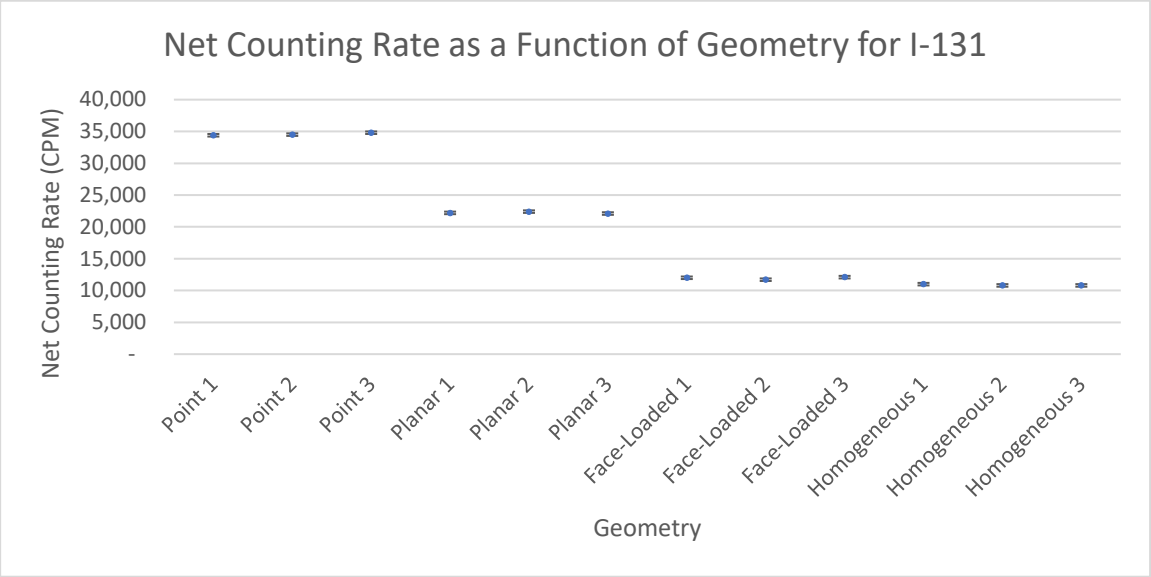

Figure 3.14. Plot showing the net counting rate (CPM) versus geometry per replicate.

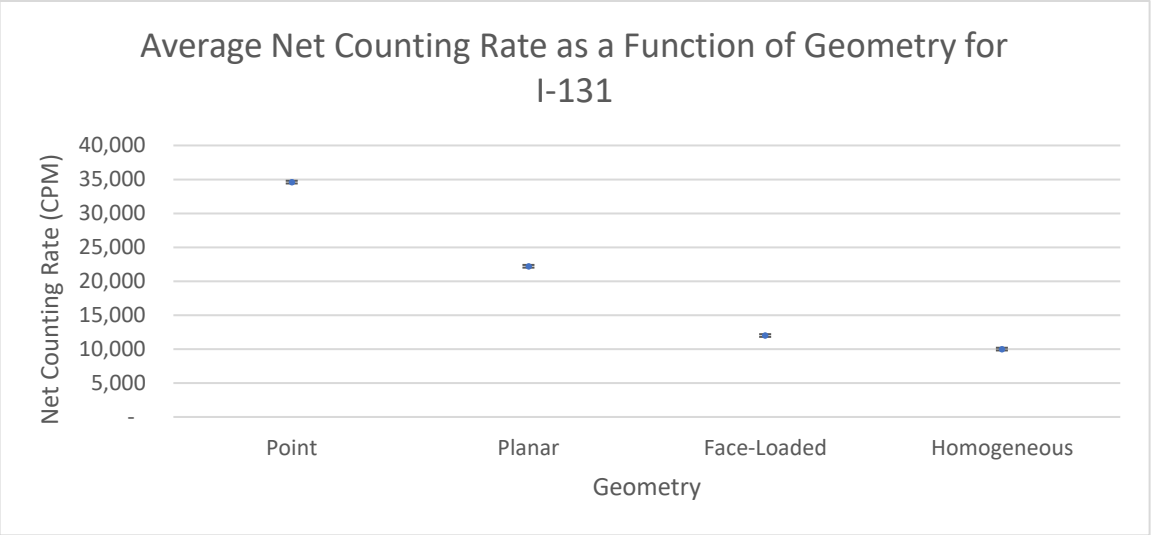

Figure 3.15. Plot showing the average net counting rate (CPM) versus geometry.

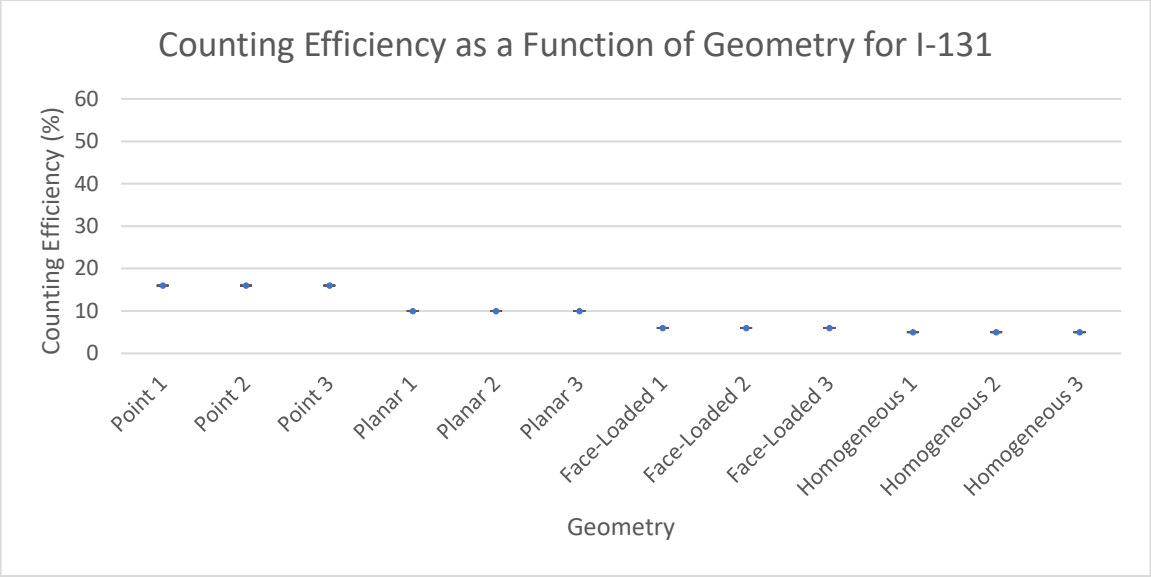

Figure 3.16. Plot showing the counting efficiency (%) versus geometry per replicate.

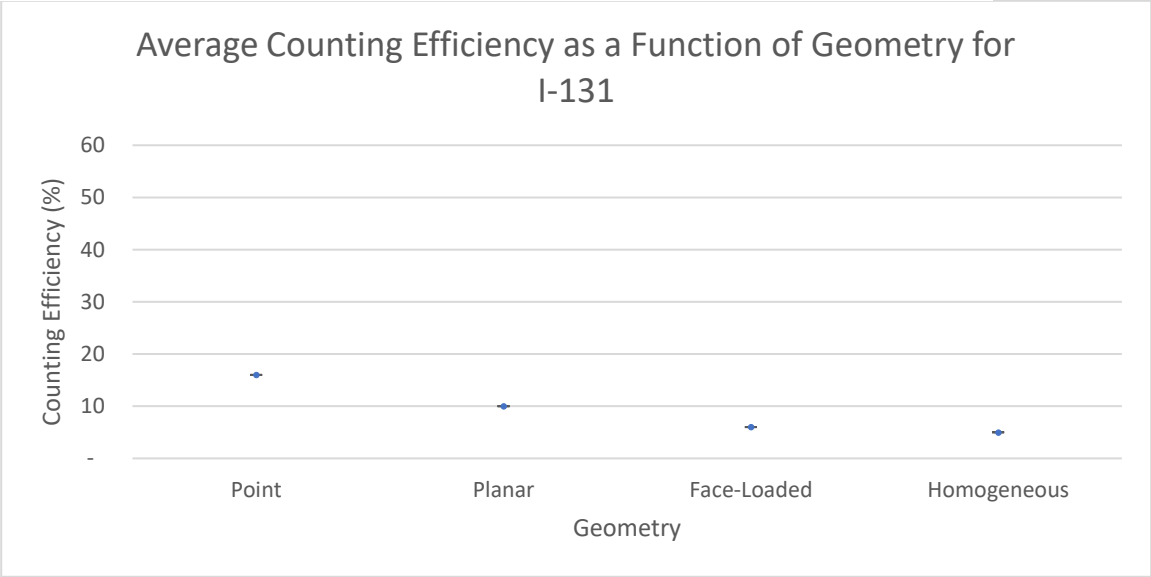

Figure 3.17. Plot showing the average counting efficiency (%) versus geometry.

3.5. Conversion Factors

With the measured net counting rates and counting efficiencies for planar, face-loaded, and homogeneous geometries for both Ba-133 and I-131, conversion factors can be calculated to correct for I-131 activities measured in the field after a nuclear incident. The equation used to calculate the activity of I-131 in the field is:

$$A\ (\mu Ci) = \frac{Measured\ Counts\ (CPM)}{\epsilon_c \left(\frac{C}{D}\right)} \times \frac{1\ min}{60\ sec} \times \frac{1\ Bq}{1\ DPS} \times \frac{1\ \mu Ci}{3{,}700\ Bq}$$

Equation 3.1.

A = activity of radioisotope in μCi,

Measured Counts = counts collected in the field in a given time,

$\in_c$ = counting efficiency of detection system based off of an Ba-133 point source in counts/disintegration.

To correct the activity in the field, the following equation would be used:

$$A\ (\mu Ci)\ \times\ conversion\ factor = corrected\ A\ (\mu Ci)$$

Equation 3.2.

$$Conversion\ factor\ = \frac{Counting\ efficiency\ for\ Ba - 133\ (point\ source)}{Counting\ efficiency\ for\ I - 131\ (FL\ or\ H)}$$

Equation 3.3.

FL = face-loaded geometry,

H = Homogeneous geometry.

To correct for activity measured in the field, the activity would have to be multiplied by the conversion factor. This would give the true activity of I-131 inside an AgZ cartridge. The conversion factor is calculated by dividing the counting efficiency of Ba-133 with point source geometry divided by the counting efficiency for I-131 using either face-loaded or homogeneous geometry. The geometry chosen by the field team would be left at their discretion. Also, for this project, the conversion factors used are determined using the measured net counting rates for face-loaded and homogeneous geometries and counting efficiencies calculated as described in

the methodology section for both Ba-133 and I-131. The table below summarizes the calculated counting efficiencies and conversion factors.

If the gaseous I-131 distribution inside the AgZ cartridge mimics face-loaded geometry:

Table 3.1. Table showing conversion factor for face-loaded geometry.

Ba-133 Calibration Geometry	Ba-133 Calculated Counting Efficiency	I-131 Calculated Counting Efficiency (Face Loaded)	Conversion Factor
Point	0.47 ± 0.02	0.06 ± 0.003	7.8 ± 0.18
Planar	0.31 ± 0.02	0.06 ± 0.003	5.2 ± 0.12

If the gaseous I-131 distribution inside the AgZ cartridge mimics homogeneous geometry:

Table 3.2. Table showing conversion factor for homogeneous geometry.

Ba-133 Calibration Geometry	Ba-133 Calculated Counting Efficiency	I-131 Calculated Counting Efficiency (Face Loaded)	Conversion Factor
Point	0.47 ± 0.02	0.05 ± 0.003	9.4 ± 0.22
Planar	0.31 ± 0.02	0.05 ± 0.003	6.2 ± 0.14

The statistical differences between the counting efficiencies for both Ba-133 and I-131 are attributed to the branching ratios for each radionuclide. In addition, there are wide variations of detection efficiency for each photon emitted by these two radionuclide using a NaI probe. Iodine-131 has higher energetic photons compared to that of Ba-133. Hence, I-131 has a lower detection efficiency, and some of the photons may be escaping the detector crystal.

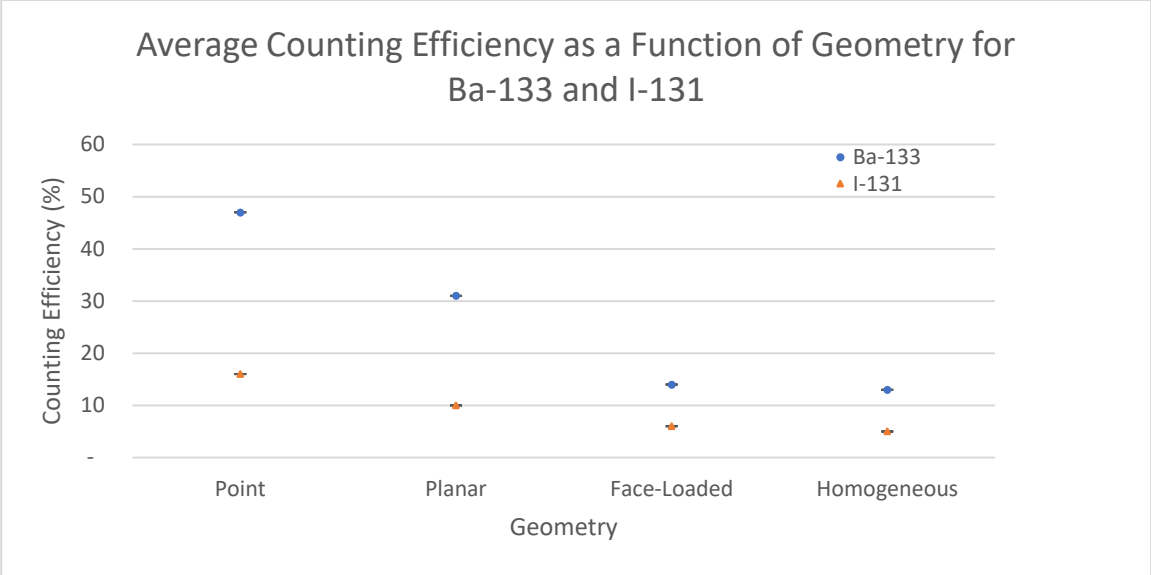

Figure 3.18. Plot showing the average counting efficiency (%) versus geometry for both Ba-133 and I-131.

CHAPTER 4. CONCLUSIONS

4.1. Phase I

As expected, there were significant differences between the net counting rates and position as to where the Ba-133 point source was placed inside the AgZ cartridge. When the source position was lowered, both the net counting rate and counting efficiency of the NaI detection system were decreased. Therefore, while calibrating a NaI detection system, position of a point source needs to be taken into consideration to mimic the geometry of the sample to be measured.

4.2. Phase II

There were significant differences in both the net counting rates and counting efficiencies between the planar, face-loaded, and homogeneous geometries using liquid Ba-133. The largest difference was between the planar and homogeneous geometries. There was a slight difference between the face-loaded and homogeneous geometries. This indicates that the photons coming off the bottom two filters for the homogeneous geometry is attenuated in the AgZ cartridge before reaching the NaI probe.

4.3. Phase III

Similar trends in decrease of net counting rates and counting efficiencies for both Ba-133 and I-131 were seen. The largest difference was between the point and homogeneous geometries. Also, as seen in phase II, there was a slight difference for both the face-loaded and homogeneous geometries. The photons coming off the bottom two filters for the homogeneous geometry was assumed to be attenuated inside the AgZ cartridge.

4.4. Conversion Factors

Conversion factors for correcting activities of I-131 in the field were calculated using the found counting efficiencies in phases II and III. This was done by dividing the counting

efficiency for Ba-133 by the counting efficiency for I-131 for face-loaded and homogeneous geometries respectively. Also, these conversion factors are geometry specific. In the field, if it is assumed that the I-131 distribution inside the AgZ cartridge is of the face-loaded geometry, then a factor of 7.8 ± 0.18 would be multiplied by the calculated I-131 activity if the NaI detection system was calibrated using a Ba-133 point source and 5.2 ± 0.12 using an planar source. If it is assumed that the I-131 distribution inside the AgZ is of the homogeneous geometry, then a factor of 9.4 ± 0.22 would be multiplied by the calculated I-131 activity if the NaI detection system was calibrated using a Ba-133 point source and 6.2 ± 0.14 using an planar source.

The use of these conversion factors would correct the I-131 activity measured inside the AgZ cartridge. The factors are straightforward to use and don't require any manipulations in the counting measurements done in the field. Also, a single Ba-133 point source can still be used to calibrate the NaI detection system. These factors are dependent on using the same NaI detection system described in the methods chapter. This entails using the same make and model for the scaler, NaI probe, and AgZ cartridge. If one does not have the same make and model for the NaI detection system, then the methodology proposed in the methods section can be utilized to derive conversion factors for different makes and models.

4.5. Future Work

The determination of conversion factors for the correction of I-131 activity after a nuclear incident has brought a strong insight into the calibration methods many agencies and institutions currently use. It is known that a single Ba-133 point source would not mimic the I-131 distribution inside an AgZ cartridge during air sampling in a plume. This project used a NaI detection system connected to a scalar to determine gross counts. This assumes that all or most of the photons coming from the source were counted for Ba-133 and I-131. The introduction of

an multi-channel analyzer (MCA) or scaler with an energy window selector can further enhance the detection of the 356 keV and 367 keV photons coming off of Ba-133 and I-131 respectively. With this information, conversion factors that are more precise may be determined to correct for the I-131 activity in a plume after a nuclear incident.

In addition, a gamma camera can be used to image a cartridge that has been used at a nuclear power plant or nuclear pharmacy producing I-131. By knowing the flow rate for the air sampler and the date at which the sample was taken, the images gathered by a gamma camera can be used to visualize whether the I-131 distribution inside the cartridge is of the face-loaded or homogeneous geometry. With this information, the field team would be able to determine what correction factor to use.

REFERENCES

Brei, T. (2013, January). NIST Traceable Calibration. Sure Controls Inc. Retrieved February 11, 2019, from Sure Controls Inc: https://www.surecontrols.com/nist-traceable-calibration/

Cember, H., Johnson, T. (2009). *Introduction to Health Physics*. New York, NY: McGraw Hill.

Cline, J. (1981, January). Retention of Noble Gases by Silver Zeolite Iodine Samples. *Health Physics*, 71-73.

Decay Schemes. Nucleonica. Retrieved February 11, 2019, from Nucleonica: https://www.nucleonica.com/wiki/index.php?title=Decay_Schemes

Gavilla, F. (2002, June). Radioiodine Collection Filter Efficiency Testing Program at F&J Specialty Products, INC. *12th Annual RETS/REMP Workshop, Atlantic City, NJ*.

Jiemwutthisak, P., Sritongkul, N., Chaudakshetrin, P., Kanchanaphiboon, P., & Tuntawiroon, M. (2012). Air Monitoring to Control the Intake of Airborne Radioiodine-131 Contaminants by Nuclear Medicine Workers. Division of Nuclear Medicine, Faculty of Medicine Siriraj Hospital, Mahidol University. *The 6th Annual Scientific Meeting, Phitsanulok, Thailand*, 85-88.

Maiello, M.L., and Hoover, M.D. (2011). *Radioactive Air Sampling Methods*. Boca Raton, FL: Taylor and Francis Group, LLC.

Montgomery, D. (1990). Calibrating Germanium Detectors for Assaying Radioiodine in Charcoal Cartridges. *Analytics Inc*, 47-51.

Radiological Accident Assessment Concepts (RAAC). Washington, DC.: Federal Emergency Management Agency. Retrieved February 11, 2019, from U.S. FEMA: https://emilms.fema.gov/IS0303/assets/CourseSummary.pdf

Radionuclide Data Sheet. *Ba-133*. Spectrum Techniques. Oak Ridge, TN. Retrieved January 22, 2019, from Spectrum Techniques: http://www.spectrumtechniques.com/wp-content/uploads/2016/12/Ba-133.pdf

Radionuclide Safety Data Sheet. *I-131*. Stanford Environmental Health and Safety. Stanford, CA. Retrieved January 22, 2019, from Stanford University: https://ehs.stanford.edu/wp-content/uploads/I-131_Inorganic.pdf

Sargis, R. (2018, October). *How Your Thyroid Works, Controlling hormones essential to your metabolism*. EndocrineWeb. Retrieved February 10, 2019, from EndocrineWeb: https://www.endocrineweb.com/conditions/thyroid/how-your-thyroid-works.

U.S. EPA. (2017, January). *PAG Manual: Protective Action Guides and Planning Guidance for Radiological Incidents*. EPA PAGs. Washington, D.C.: U.S. Environmental Protection Agency. Retrieved January 22, 2019, from U.S. EPA: https://www.epa.gov/sites/production/files/2017-01/documents/epa_pag_manual_final_revisions_01-11-2017_cover_disclaimer_8.pdf

U.S. NRC. (1980, November). *Criteria for Preparation and Evaluation of Radiological Emergency Response Plans and Preparedness in Support of Nuclear Power Plants*. NUREG-0654. Washington, D.C.: U.S. Nuclear Regulatory Commission. Retrieved January 22, 2019, from U.S. NRC: https://www.nrc.gov/docs/ML0404/ML040420012.pdf.

U.S. NRC. (2017). *Map of Power Reactor Sites*. Washington, D.C.: U.S. Nuclear Regulatory Commission. Retrieved February 11, 2019, from U.S. NRC: https://www.nrc.gov/reactors/operating/map-power-reactors.html

Wang, W-H., Matthews II, K.L. (2006, May). Simulating Gaseous ^{131}I Distribution in a Silver Zeolite Cartridge Using Sodium Iodide Solution. *Health Physics*, S73-S79.

VITA

Amin Hamideh was born in Chicago, IL in 1983. He was raised most of his life in Baton Rouge, LA. Amin attended Broadmoor Senior High School and graduated in 2002. He then entered Louisiana State University (LSU) and graduated with a bachelor's degree in biochemistry in 2007. Amin then worked for a laboratory at LSU conducting research in protein X-ray crystallography. In 2010, Amin returned to LSU to obtain a bachelor's degree in physics with a concentration in health physics. Amin graduated from LSU with his second bachelor's degree in 2012. In 2013, he began work at the Radiation Safety Office at LSU where he still resides. His job duties include: radiation use application review, radioactive waste management, radiation monitoring equipment management, conducting laboratory audits and surveys, performing leak tests on sealed sources, as well as training new radiation workers. Amin passed Part I of the American Board of Health Physics examination and plans on taking Part II in Summer 2019 to obtain board certification as a health physicist.